

Degeneracy & White Dwarfs

The electrons obey Fermi statistics which are normally treated parametrically with both the electron density N_e and the electron pressure P_e given as functions of a degeneracy parameter $\alpha = -\mu/kT$ and the temperature T . The general expression for the electron density is:

$$N_e(p_x, p_y, p_z) = \frac{g}{(2\pi\hbar)^3} \frac{dp_x dp_y dp_z}{\exp[(-\mu + \epsilon)/kT] + 1} \quad (1)$$

or in terms of dp :

$$N_e(p) dp = \frac{g}{(2\pi\hbar)^3} \frac{4\pi p^2 dp}{\exp[(-\mu + \epsilon)/kT] + 1} \quad (2)$$

where α or μ must be adjusted until the total number of electrons is that given by the density: $N_e = \frac{1}{\mu_e} \frac{\rho}{m_U}$ with $\frac{1}{\mu_e} = X + \frac{1}{2}Y + \frac{1}{2}Z = \frac{1}{2}(1 + X)$ and g is the degeneracy of the Fermion due to its internal spin I and for the electron with $I = 1/2$ we get $g = 2$.

The pressure is the flux of momentum across a surface. Both the momentum and surface define a direction and this direction is the same for both in an isotropic gas. A representative expression for this flux of momentum is $p_x v_x$ which after averaging is equivalent to $\frac{1}{3}p v_p$ where p is the absolute value of the momentum and v_p is the corresponding absolute value of the velocity.

Expressing the total N_e and P_e as integrals over p we have

$$N_e = \frac{g}{2\pi^2\hbar^3} \int_0^\infty \frac{p^2 dp}{\exp[(-\mu + \epsilon)/kT] + 1} = \frac{g}{2\pi^2\hbar^3} \int_0^\infty \frac{p^2 dp}{\exp(\alpha + \epsilon/kT) + 1} \quad (3)$$

and

$$P_e = \frac{g}{6\pi^2\hbar^3} \int_0^\infty \frac{p^3 v_p dp}{\exp[(-\mu + \epsilon/kT)] + 1} = \frac{g}{6\pi^2\hbar^3} \int_0^\infty \frac{p^3 v_p dp}{\exp(\alpha + \epsilon/kT) + 1} \quad (4)$$

where $\alpha = -\mu/kT$. As N_e increases, α becomes more negative and μ more positive. A common alternate notation is to use $\psi = -\alpha = \mu/kT$ and this is the quantity which has been used to label the degeneracy on various ρ vs. T diagrams.

Degeneracy continued

In order to proceed we need to express the velocity v_p in terms of the electron mass m_e and the momentum p . We first take the limiting case of non-relativistic energies and use

$$v_p = \frac{p}{m_e} \quad (5)$$

After replacing p by a dimensionless energy $u = p^2/2m_e kT$ the density and pressure can be written:

$$P_e = \frac{8\pi kT}{3h^3} (2m_e kT)^{3/2} F_{3/2}(\alpha) \quad (6)$$

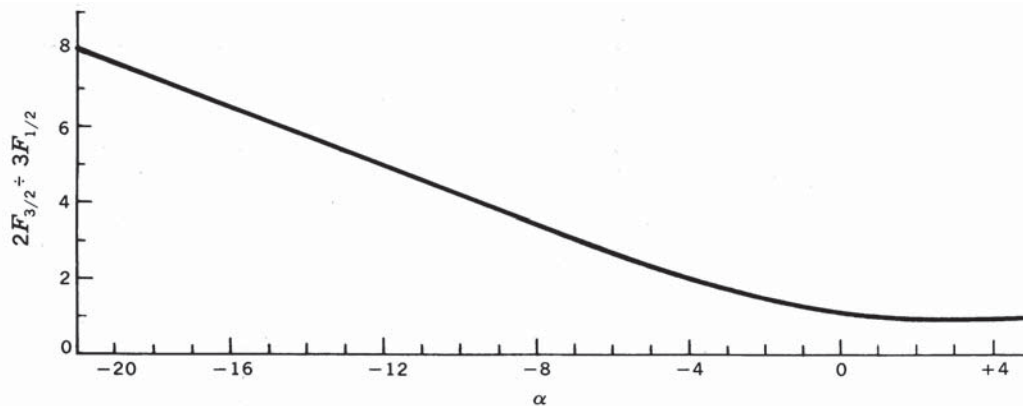
and

$$N_e = \frac{4\pi}{h^3} (2m_e kT)^{3/2} F_{1/2}(\alpha) \quad (7)$$

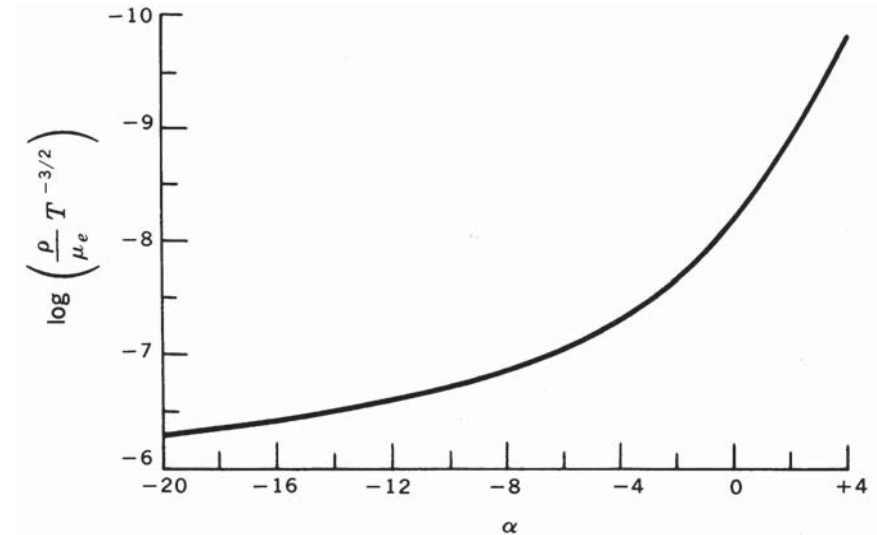
where $F_{1/2}(\alpha)$ and $F_{3/2}(\alpha)$ are called the Fermi-Dirac functions and are given by:

$$F_{1/2} = \int_0^\infty \frac{u^{1/2} du}{\exp(\alpha + u) + 1} \quad \text{and} \quad F_{3/2} = \int_0^\infty \frac{u^{3/2} du}{\exp(\alpha + u) + 1} \quad (8)$$

These functions are tabulated in various locations. The two figures below illustrate some of the more interesting properties of the functions:



This figure shows the ratio of pressure of a degenerate gas to what it would have if the velocities were Maxwellian (non-degenerate).



This figure shows the relationship between the degeneracy parameter α and the density of electrons.

Complete Degeneracy

In the case of α a large negative number, the denominator is unity until $u > -\alpha$ and then the denominator becomes zero. The momentum at this energy is

$$p_0 = (-\alpha 2m_e kT)^{1/2} \quad (9)$$

We can now replace the integrals to ∞ by integrals to p_0 and set the denominator to 1 for $p < p_0$. For the non-relativistic case this gives:

$$P_e = \frac{8\pi}{15m_e h^3} p_0^5. \quad (10)$$

For the extreme relativistic case we can replace v_p by c to get

$$P_e = \frac{2\pi c}{3h^3} p_0^4. \quad (11)$$

Using the expression for the N_e in terms of the density we can express P_e numerically as:

$$P_e = K_1 \left(\frac{1}{\mu_e} \rho \right)^{5/3} \quad (\text{Non-Relativistic}) \quad (12)$$

$$P_e = K_2 \left(\frac{1}{\mu_e} \rho \right)^{4/3} \quad (\text{Relativistic}) \quad (13)$$

with

$$K_1 = 7 \frac{h^2}{20m_e m_U} \left(\frac{3}{\pi m_U} \right)^{2/3} = 9.91 \times 10^{12} \quad (14)$$

and

$$K_2 = \frac{hc}{8m_U} \left(\frac{3}{\pi m_U} \right)^{1/3} = 1.23 \times 10^{15} \quad (15)$$

Arbitrary Degeneracy

In general it is necessary to use

$$v_p = \frac{\partial E}{\partial p} \quad (16)$$

Where E is the kinetic energy. This function in general is:

$$\frac{\partial E}{\partial p} = \frac{1}{m_e} \left(1 + \frac{p^2}{m_e^2 c^2} \right)^{-1/2} p \quad (17)$$

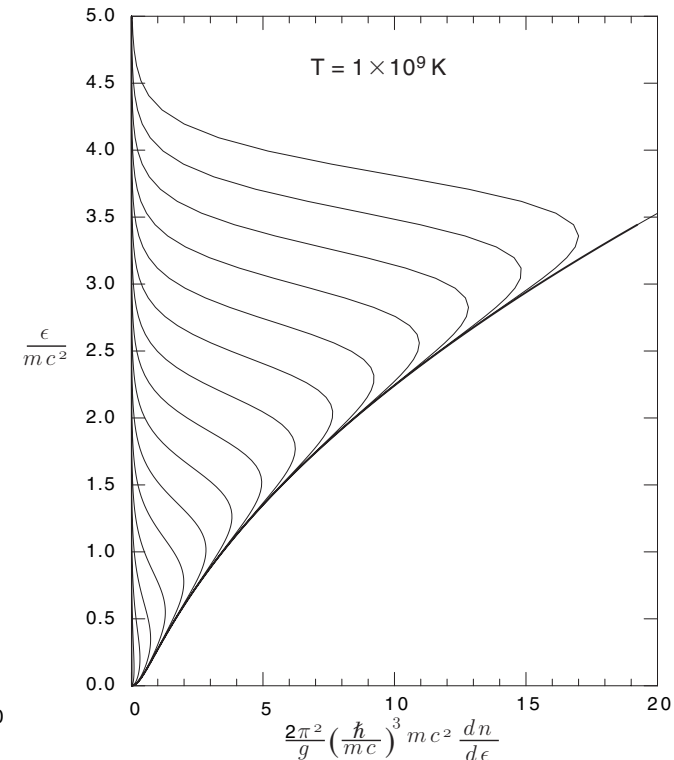
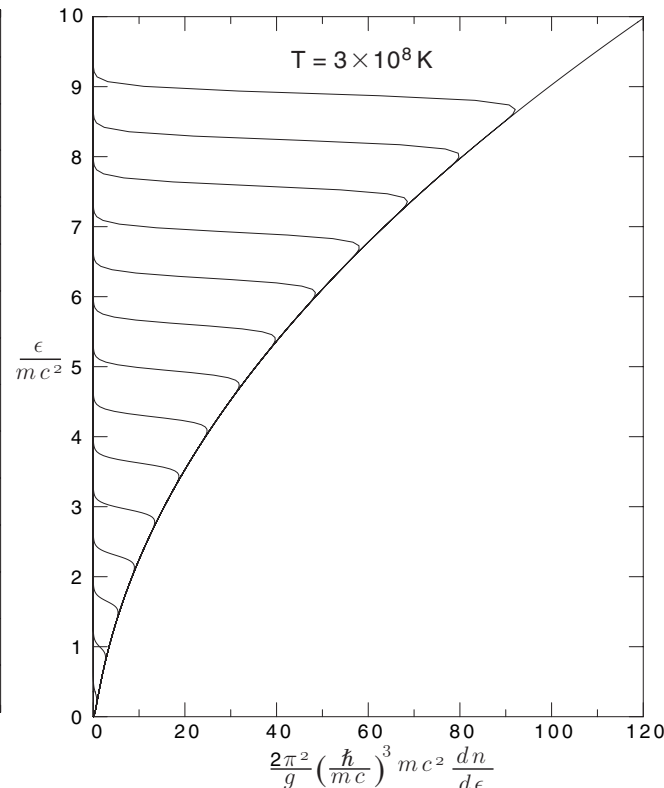
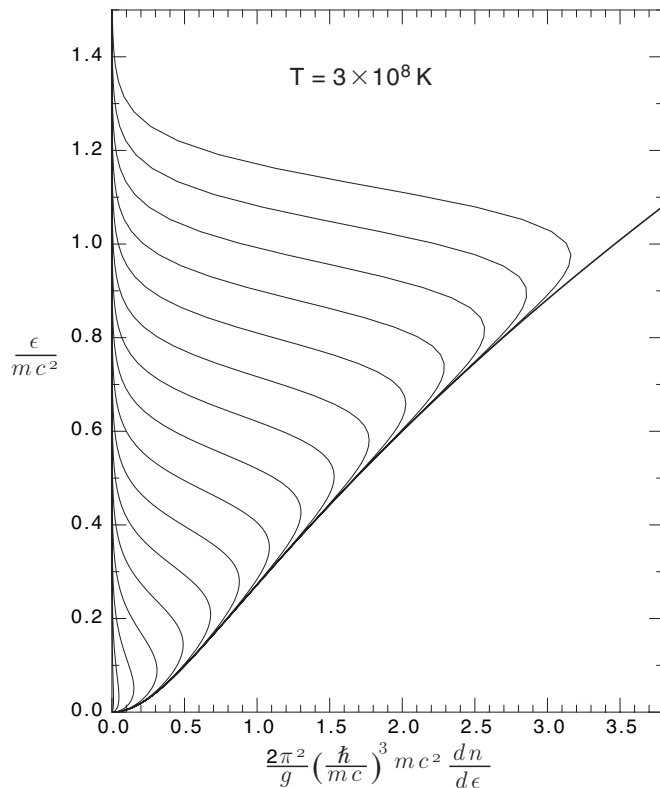
Build-up of Degeneracy

It is worth looking at the shape of the phase space volume as the electron energy increases and the relativistic mass-momentum equation involves the speed of light limit. Let us look at the density of states n as a function of electron kinetic energy ϵ and in particular examine $dn/d\epsilon$. This is

$$\frac{dn}{d\epsilon} = \frac{g}{2\pi^2 \hbar^3} \frac{p^2 dp/d\epsilon}{\exp[(\epsilon - \mu)/kT] + 1} = \frac{g}{2\pi^2 mc^2} \left(\frac{mc}{\hbar}\right)^3 \frac{\tilde{p}^2 d\tilde{p}/d\tilde{\epsilon}}{\exp[\Phi(\tilde{\epsilon} - \tilde{\mu})]} \quad (18)$$

where $\Phi = \frac{mc^2}{T} = \frac{5.9 \times 10^9 \text{ K}}{T}$, $\tilde{p} = \frac{p}{mc}$ and $\tilde{\epsilon} = \frac{\epsilon}{mc^2}$. The kinetic energy and momentum are then related by:

$$\epsilon + mc^2 = (p^2 c^2 + m^2 c^4)^{1/2} \quad \text{or} \quad \tilde{p} = [(\tilde{\epsilon} + 1)^2 - 1]^{1/2} \quad \text{and} \quad \tilde{p}^2 \frac{d\tilde{p}}{d\tilde{\epsilon}} = (\tilde{\epsilon} + 1) [(\tilde{\epsilon} + 1)^2 - 1]^{1/2} \quad (19)$$



White Dwarfs

Using:

$$P = \frac{8\pi}{3h^3} \int_0^{p_0} p^3 \frac{\partial E}{\partial p} dp \quad (20)$$

and

$$\frac{\partial E}{\partial p} = \frac{1}{m_e} \left(1 + \frac{p^2}{m_e^2 c^2}\right)^{-1/2} p, \quad E = m_e c^2 \left\{ \left(1 + \frac{p^2}{m_e^2 c^2}\right)^{1/2} - 1 \right\} \quad (21)$$

we can write for the pressure due to the electrons:

$$P = \frac{8\pi}{3m_e h^3} \int_0^{p_0} \frac{p^4 dp}{\left(1 + \frac{p^2}{m_e^2 c^2}\right)^{1/2}}. \quad (22)$$

This integral can be done analytically by using the substitutions $\sinh\theta = \frac{p}{m_e c}$ and $\sinh\theta_0 = \frac{p_0}{m_e c}$ to give:

$$P = \frac{8\pi m_e^4 c^5}{3h^3} \int_0^{\theta_0} \sinh^4\theta d\theta \quad (23)$$

to obtain the result:

$$P = \frac{\pi m_e^4 c^5}{3h^3} f(x) = 6.01 \times 10^{22} f(x) \equiv A f(x) \quad (1)$$

where $x = \frac{p_0}{m_e c}$ and

$$f(x) = x(2x^2 - 3)(x^2 + 1)^{1/2} + 3\sinh^{-1}x. \quad (24)$$

Using the relationship between p_0 and ρ from before and adding the definition of x we get:

$$\rho = \frac{8\pi}{3h^3} M_U \mu_e (m_e c x)^3 = 9.82 \times 10^5 \mu_e x^3 \equiv B x^3. \quad (25)$$

These two equations complete the parametric representation of the equation of state at zero T . It is accurate at all densities as long as the electrons remain at low enough energies that they do not combine with the protons to form neutrons.

Application to Hydrostatic Equilibrium and Mass Distribution

We can carry out an analysis similar to that which we used to derive the polytrope equations since we have as before a relationship between ρ and P which is independent of T . Thus we again do not need to invoke the energy generation and energy transport equations to get a closed system. The equation expressing hydrostatic equilibrium and mass distribution is:

$$\frac{1}{r^2} \frac{d}{dr} \left(\frac{r^2}{\rho} \frac{dP}{dr} \right) = -4\pi G \rho . \quad (26)$$

This is converted to an equation in x by inserting the parametric representation of both variables from the previous page. Since P appears inside various derivatives, it is advantageous to use the representation of P in terms of the integral: $P = 8A \int_0^{\theta_0} \sinh^4 \theta d\theta$. The derivative $\frac{dP}{dr}$ can be expanded with the chain rule to $\frac{dP}{d\theta_0} \frac{d\theta_0}{dx} \frac{dx}{dr}$. The first two derivatives are:

$$\frac{dP}{d\theta_0} = 8Ax^4 \quad , \quad \frac{d\theta_0}{dx} = (x^2 + 1)^{-1/2} \quad (27)$$

so that the H.E. + M.D. equation becomes:

$$\frac{8A}{B} \frac{1}{r^2} \frac{d}{dr} \left[\frac{r^2}{x^3} \frac{x^4}{(x^2 + 1)^{1/2}} \frac{dx}{dr} \right] = -4\pi GBx^3 . \quad (28)$$

Using the fact that $\frac{x dx}{(x^2+1)^{1/2}} = d(x^2 + 1)^{1/2}$ and replacing $x^2 + 1$ with y^2 this equation becomes:

$$\frac{1}{r^2} \frac{d}{dr} \left(r^2 \frac{dy}{dr} \right) = -\frac{\pi GB^2}{2A} (y^2 - 1)^{3/2} . \quad (29)$$

This looks like the Lane-Emden equation with $n = 3$ for $y \gg 1$ and with $n = 3/2$ for $y \approx 1$ (i.e. $x^2 \ll 1$). Note however that the central boundary condition on y is related to the central density rather than being arbitrary as it was for the polytrope. The different configurations are also not homology transformations of each other.

Polytrope-like Transformations

To exhibit the properties of the solutions, it is useful to carry out transformations like those used to simplify the study of the polytropes. To get a function which is unity at $r = 0$ define $\phi = \frac{y}{y_0}$. Next stretch the r coordinates so that the dimensional terms are canceled out: $r = \alpha\eta$ with

$$\alpha = \left(\frac{2A}{\pi G}\right)^{1/2} \frac{1}{By_0} \quad (30)$$

to get the equation:

$$\frac{1}{\eta^2} \frac{d}{d\eta} \left(\eta^2 \frac{d\phi}{d\eta} \right) = - \left(\phi^2 - \frac{1}{y_0^2} \right)^{3/2} \quad (31)$$

Note that as ρ_0 and $y_0 \rightarrow \infty$, $\alpha \rightarrow 0$. This implies that unless the solution has $\eta \rightarrow \infty$ faster than $\alpha \rightarrow 0$, the degenerate star radius becomes zero at high central densities.

Following the same approach we used to get the mass of the polytrope, we can use the hydrostatic equilibrium equation here.

$$\frac{dP}{dr} = -\frac{GM_r}{r^2} \rho \quad (32)$$

or

$$\begin{aligned} \frac{8Ax^4}{(x^2+1)^{1/2}} \frac{dx}{dr} &= -\frac{Bx^3GM_r}{r^2} \\ -\frac{8A}{BG} r^2 \frac{d(x^2+1)^{1/2}}{dr} &= M_r \end{aligned} \quad (33)$$

$$M_r = -\frac{8A}{GB} \left(\frac{2A}{\pi G}\right)^{1/2} \frac{1}{By_0} \eta^2 \frac{dy}{d\eta} \quad (34)$$

$$= -4\pi \left(\frac{2A}{\pi G}\right)^{3/2} \frac{1}{B^2} \eta^2 \frac{d\phi}{d\eta} \quad (35)$$

Low Density Limit

For small x_0 we have the low density case of the white dwarf. In this case we can replace y_0 and y_0^2 by approximate results:

$$y_0 \approx 1 + \frac{x_0^2}{2}, \quad \frac{1}{y_0^2} \approx 1 - x_0^2 \tag{36}$$

and expand ϕ . Define a new variable θ by:

$$\theta = \phi^2 - \frac{1}{y_0^2} = (\phi^2 - 1) - (1 - x_0^2) + 1 \approx 2\phi - 2 + x_0^2 \tag{37}$$

After stretching the coordinates again by $\xi = \sqrt{2}\eta$ the equation becomes:

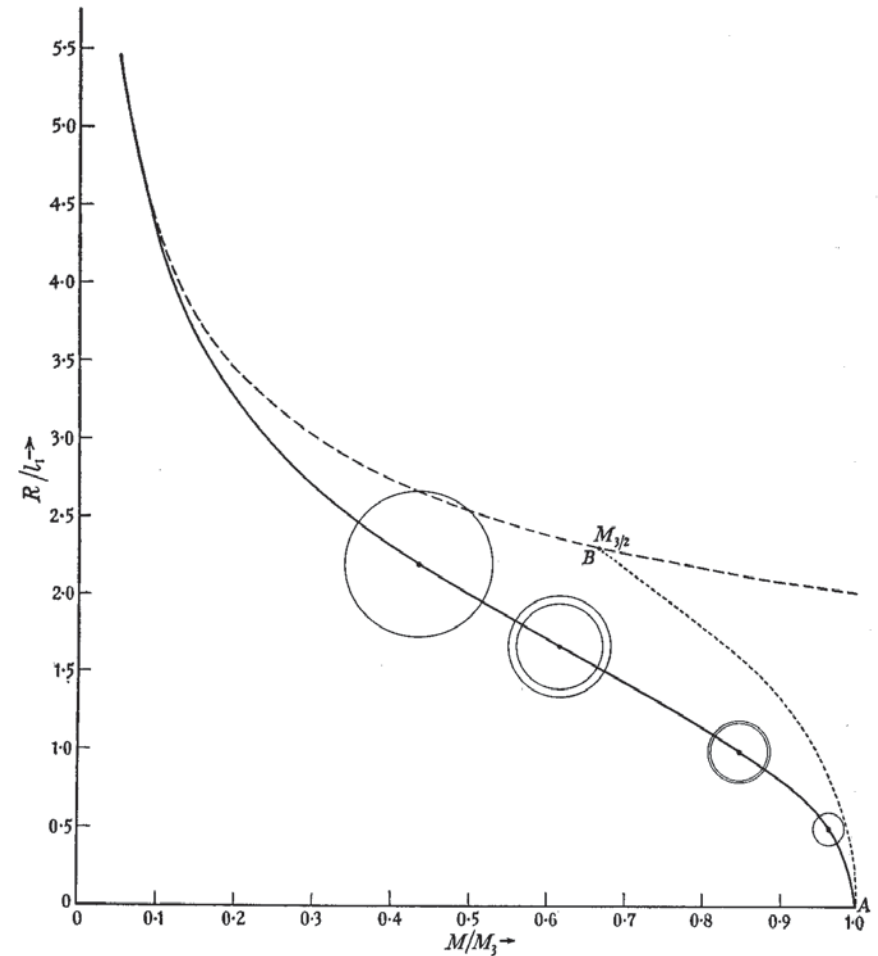
$$\frac{1}{\xi^2} \frac{d}{d\xi} \left(\xi^2 \frac{d\theta}{d\xi} \right) = -\theta^{3/2} \tag{38}$$

which is the Lane-Emden equation. The central boundary condition is that $\theta(\xi = 0) = x_0^2$ instead of unity.

General Results

THE PHYSICAL CHARACTERISTICS OF COMPLETELY DEGENERATE CONFIGURATIONS

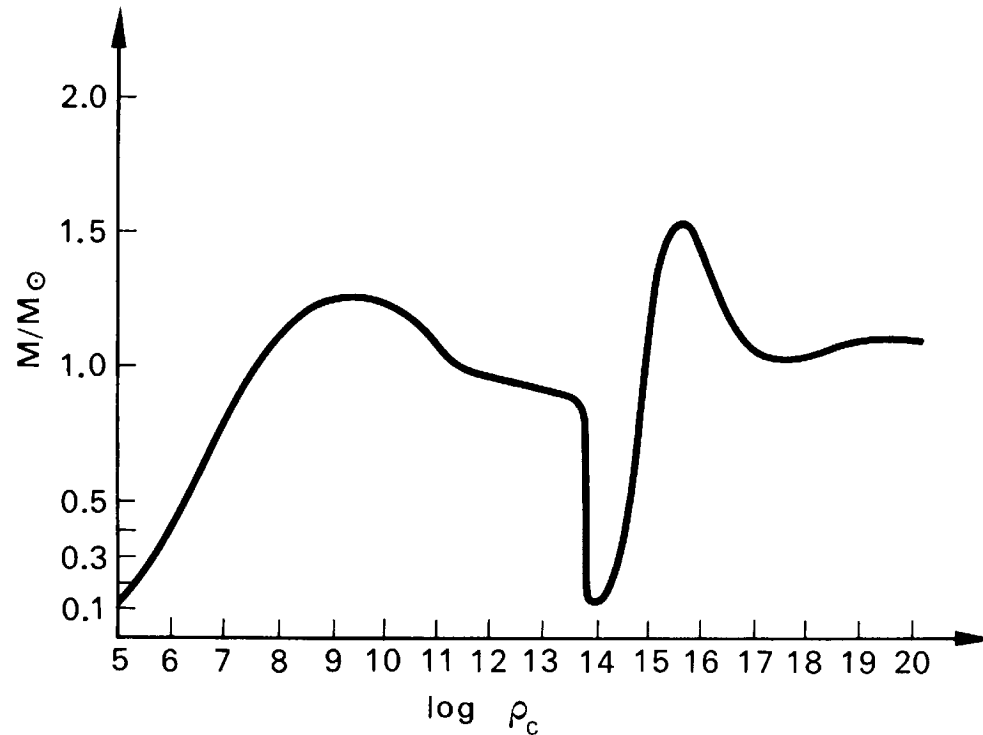
$1/y_0^2$	M/\odot	ρ_0 in Grams per Cubic Centimeter	ρ_{mean} in Grams per Cubic Centimeter	Radius in Centimeters
0.....	5.75	∞	∞	0
0.01.....	5.51	9.67×10^8	3.70×10^7	4.13×10^8
0.02.....	5.32	3.37×10^8	1.57×10^7	5.44×10^8
0.05.....	4.87	8.13×10^7	5.08×10^6	7.69×10^8
0.1.....	4.33	2.65×10^7	2.10×10^6	9.92×10^8
0.2.....	3.54	7.85×10^6	7.9×10^5	1.29×10^9
0.3.....	2.95	3.50×10^6	4.04×10^5	1.51×10^9
0.4.....	2.45	1.80×10^6	2.29×10^5	1.72×10^9
0.5.....	2.02	9.82×10^5	1.34×10^5	1.93×10^9
0.6.....	1.62	5.34×10^5	7.7×10^4	2.15×10^9
0.8.....	0.88	1.23×10^5	1.92×10^4	2.79×10^9
1.0.....	0	0	0	∞



* The values given in this table differ slightly from the published values (S. Chandrasekhar *M.N.*, 95, 208, 1935, Table III). The difference is due to the change in the accepted values of the fundamental physical constants. The calculations are for $\mu_e = 1$. For the other values of μ_e , M should be multiplied by μ_e^{-2} , R by μ_e^{-1} , and ρ_0 by μ_e .

Beyond the White Dwarf Limit

The central density defines the model as long as the temperature is effectively zero. For each central density there is a specific model having a specific total mass. This trend is illustrated below:



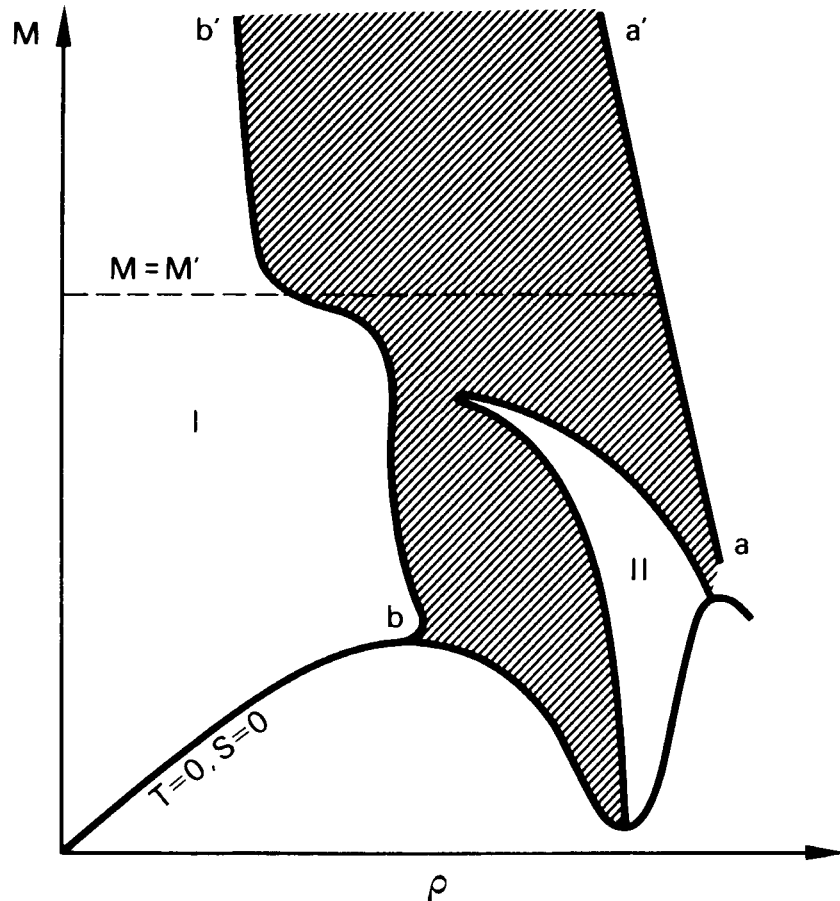
This figure illustrates the mass of a $T = 0$ model as a function of the central density

Note the following:

- The maximum mass in the white dwarf section does not quite reach the Chandrasekhar mass. This is due to the fact that as the density approaches infinity, it encounters other factors which introduce a limit.
- Above the mass limit, the mass of the model decreases as the central density increases. This means that in fact there are no stable models in this range.
- The last set of stable models correspond to neutron stars.

The Effect of Non-Zero Temperature on Stable Models

When the temperature is high enough to increase the pressure, it is possible to have higher mass models at the specified central densities. This is illustrated below where the non-zero temperature is parameterized by the entropy of the gas:



With the finite temperature a new range of stable masses is possible:

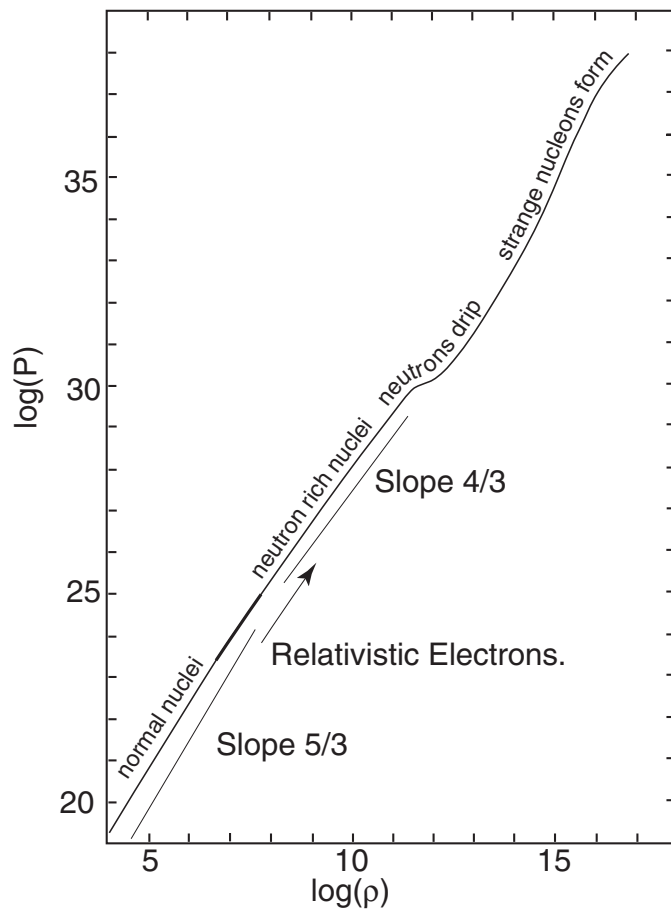
- The excursion near the white dwarf limit represents those models with a high enough temperature to support the extra mass.
- The boundary on the right represents the formation of Black Holes.

Masses as a function of central density when the matter is hot.

High Density Equation of State

After the density passes the range where the electrons become degenerate, they eventually have a high enough energy that they can reverse β decays that normally occur to bring the nuclei to the balance of neutrons and protons found in free matter. This produces neutron rich nuclear matter and reduces the number of electrons per gram of mass. Eventually the nuclei become so neutron rich that some neutrons are expelled from the nuclei. This is called "Neutron Drip" and results in the creation of a free neutron sea. When this neutron gas becomes degenerate, the pressure again increases to give a neutron star equation of state. These effects are illustrated below:

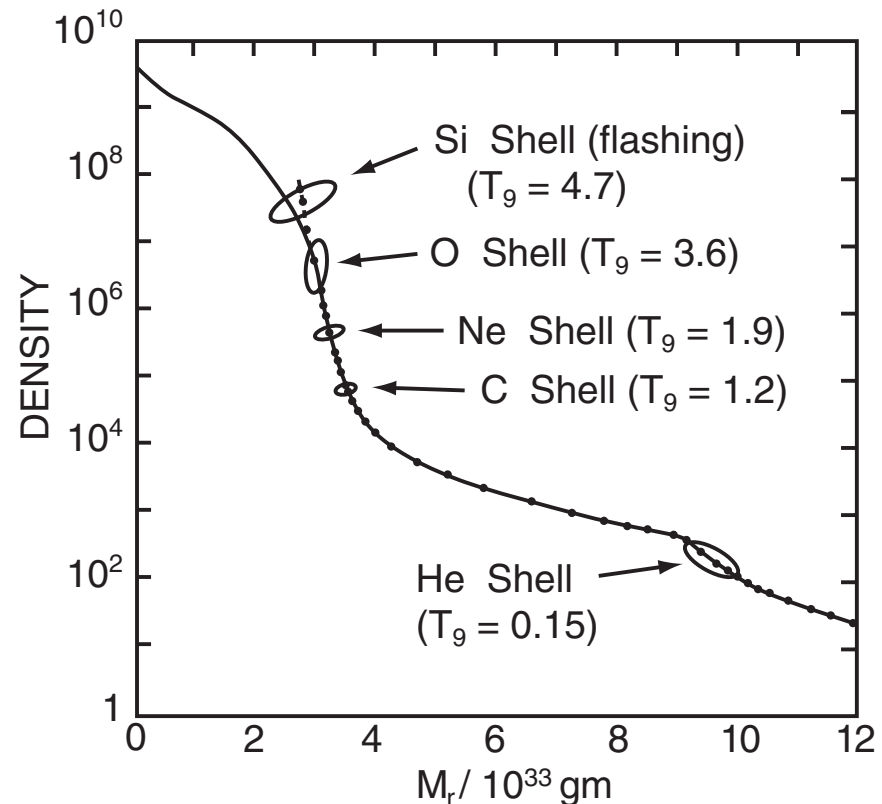
Neutron Star Pressure Function

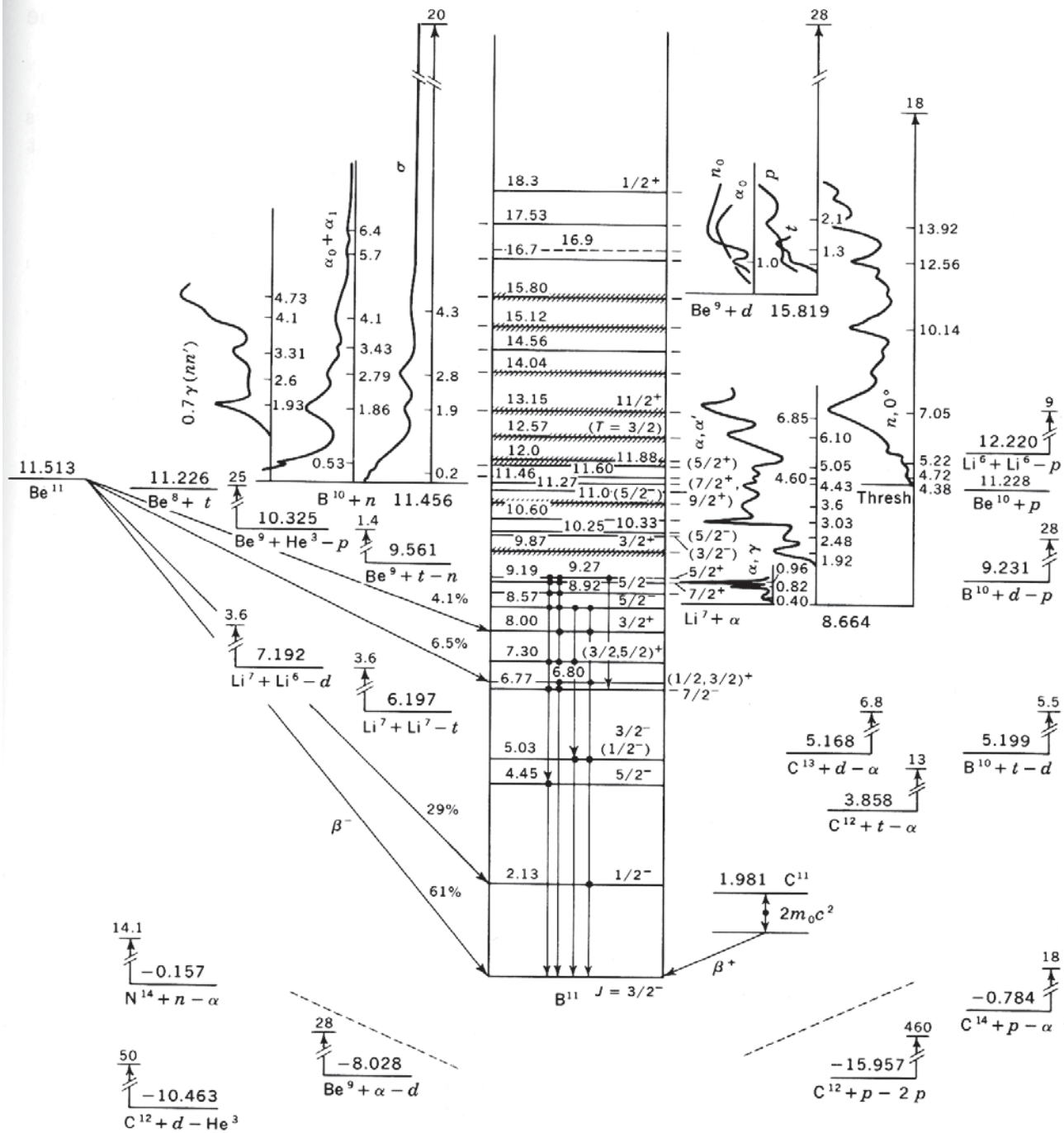


The equation of state for cold matter at neutron star densities.

Approach to Core Collapse in a Supernova

In a star with a core where the mass is so high that the central parts begin to approach the collapse point the structure is like that below:



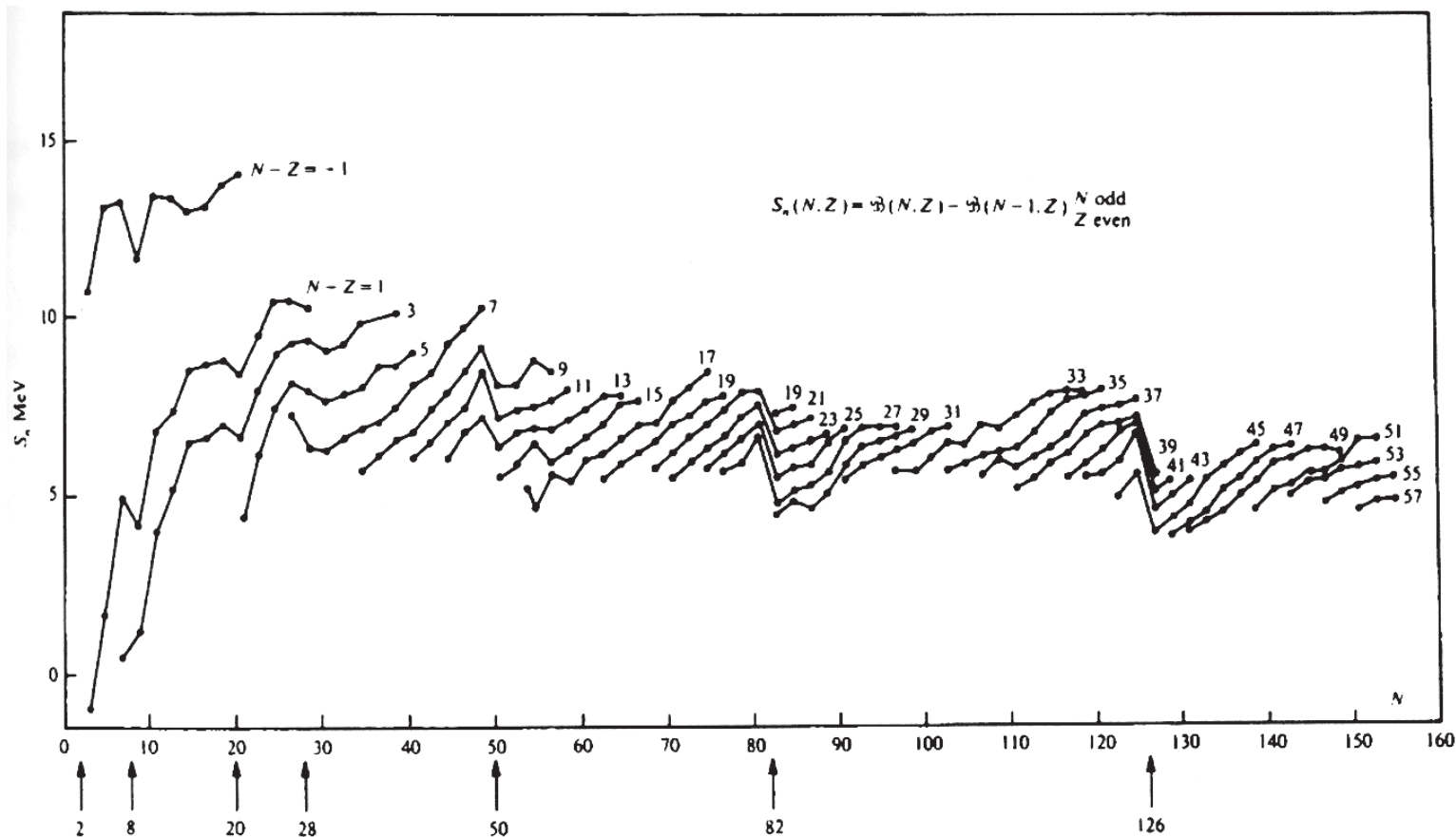


An Example of a Nuclear Energy Diagram ^{11}B

This figure has its energy levels set at zero for the ground state of ^{11}B . Internal states with different nuclear angular momentum and parity are indicated. To each side are shown the various combinations of particles with their zero points adjusted so that if they are combined into ^{11}B , the energy released or absorbed is indicated.

Of interest is the neutron separation energy of 11.456 MeV. This is a measure of the nuclear binding. In this case, the ^{11}B nucleus has 5 protons and 6 neutrons so that the neutrons are paired prior to the removal of one. This even-odd effect increases the binding energy of the neutron.

The Nuclear Shell Structure

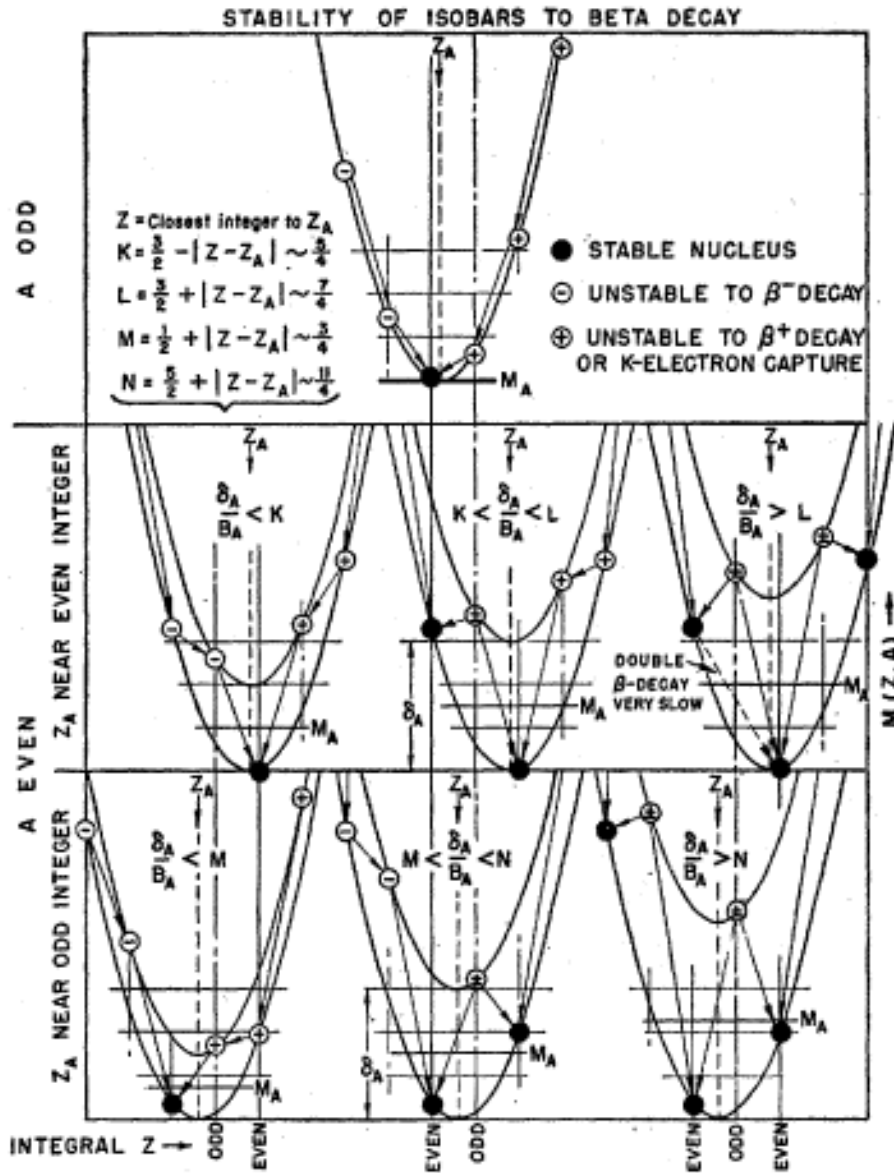


The above figure shows the energy required to remove one neutron from each nucleus. These separation energies have been corrected for the systematic even-odd effect. The abscissa is the neutron number while each line is labeled by the neutron number N minus the proton number Z .

The closed shells are shown by the arrows along the bottom. The neutron which is one in excess of the closed shell number is more weakly bound as shown and this effect is enhanced because each also has been corrected by the even-odd effect which further weakens the binding energy.

Nuclei with the closed shell number of neutrons systematically do not absorb an additional neutron during r -process nucleosynthesis.

The Dependence of Nuclear Energy On Z at Fixed A



- Even-Odd** These have odd A and follow a single systematic pattern.
- Even-Even** These have highest energy protons and neutrons spin paired and have lower energy.
- Odd-Odd** These have highest energy protons and neutrons spin unpaired and have higher energy.

Effect of Electrons at High Density on Nuclear Stability

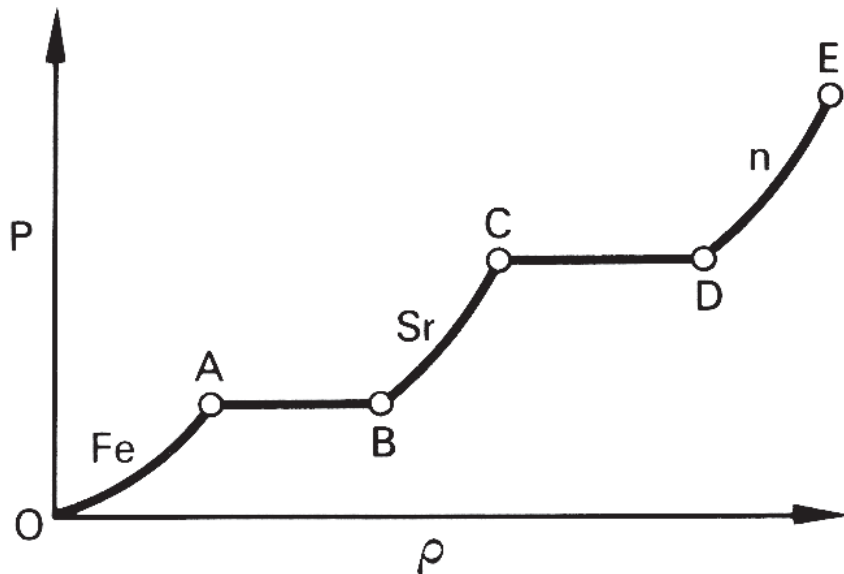
CRITICAL POINTS FOR THE TRANSITIONS
BETWEEN DIFFERENT NUCLEI

Z	A	E_F	$\log_{10} \rho$
26.....	56
28.....	62	0.6	7.15
28.....	64	2.5	8.63
28.....	66	3.9	9.15
28.....	68	6.1	9.69
30.....	76	7.0	9.87
30.....	78	8.5	10.13
30.....	80	9.5	10.28
32.....	90	14.8	10.84
38.....	120	20.6	11.28
n	1	24.0	11.53

As the energy of the electrons at the top of the Fermi distribution rises as the density is increased, the electrons have more energy than is needed to force an inverse β decay and convert one of the protons to a neutron thus reducing the nuclear charge. If the temperature is high enough to permit the nuclei to approach nuclear thermodynamic equilibrium so that the most stable nucleus is formed, the result will be to shift the most stable species to higher mass with a greater excess of neutrons than is found at lower density. The first shift from this process is to make ^{62}Sr more abundant than the ^{56}Fe . The progression of these changes is shown in the table to the left.

The diagram below the table shows how the increase in pressure is slowed by virtue of the absorption of the electrons into the nuclei. The stretch from **A** to **B** is where the Fe is being converted to Sr. The stretch from **C** to **D** is where the neutrons are dripping out of the nuclei.

This table and figure are from Zeldovich and Novikov, *Relativistic Astrophysics, Vol. 1, Stars and Relativity*.



Systematics of Nucleosynthesis

REVIEWS OF

MODERN PHYSICS

VOLUME 29, NUMBER 4

OCTOBER, 1957

Synthesis of the Elements in Stars*

E. MARGARET BURBIDGE, G. R. BURBIDGE, WILLIAM A. FOWLER, AND F. HOYLE

*Kellogg Radiation Laboratory, California Institute of Technology, and
Mount Wilson and Palomar Observatories, Carnegie Institution of Washington,
California Institute of Technology, Pasadena, California*

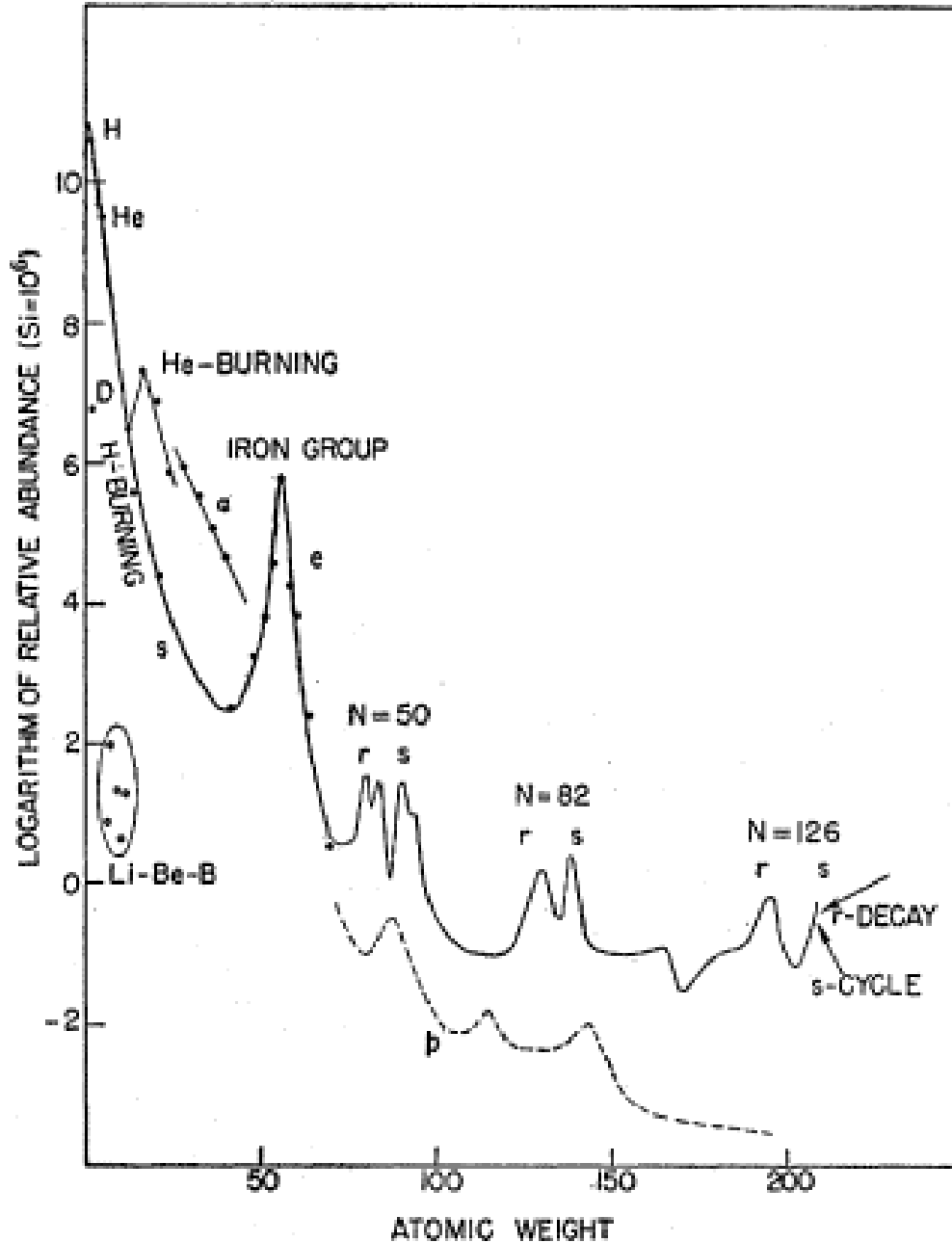
“It is the stars, The stars above us, govern our conditions”;
(King Lear, Act IV, Scene 3)

but perhaps

“The fault, dear Brutus, is not in our stars, But in ourselves,”
(Julius Caesar, Act I, Scene 2)

This paper set the groundwork for much of nuclear astrophysics. It developed rapidly from the first determination of abundances of the elements in the universe as presented by Suess and Urey (1956RMP...28..53S). The patterns seen in these abundances demanded rather directly that the primary nucleosynthesis processes include the α -process, the e-process, the s-process, the r-process and the p-process.

The Abundances Summarized by Suess and Urey



The abundance pattern has been smoothed but the principal features are marked. The hydrogen starting point is at the left with a series of higher than average species being formed by multiples of the helium nucleus or α particle. The big peak near ^{56}Fe is due to that nucleus being the most stable and for there having operated a process that brings the nuclear abundances toward the nuclear thermodynamic equilibrium values. The s-process involves slowly adding neutrons to the iron peak elements while the r-process involves adding neutrons quickly to the iron peak nuclei.

Hydrogen Burning When protons are available at high enough temperature, their capture moves the product nucleus to the right on this figure. Neutron addition, if it occurs for the lighter nuclei, is also shown as a rightward shift. These processes normally occur during main sequence evolution but under some circumstances can also take place in evolved stars.

Helium Burning The primary process is the 3- α reaction to form ^{12}C followed by the formation of ^{16}O , ^{20}Ne and ^{24}Mg as indicated along the left side of the figure. Other CNO nuclei can undergo similar α addition reactions, often with the emission of a neutron.

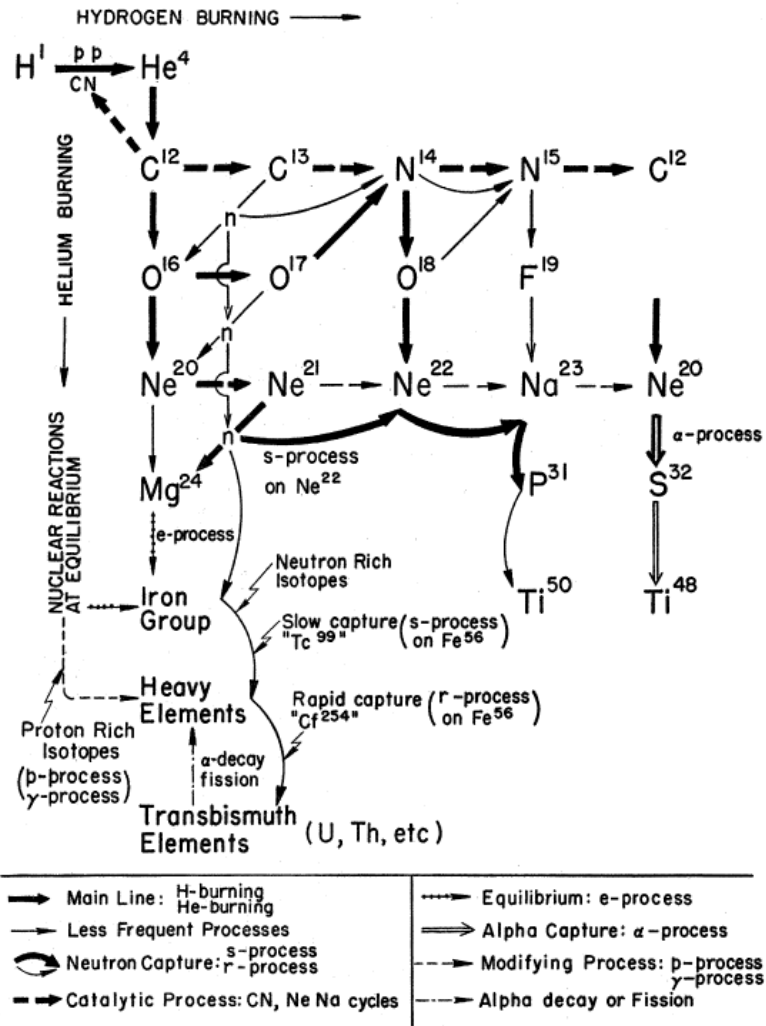
α -process This is similar to regular helium burning but occurs at a higher temperature so that the Coulomb repulsion no longer discriminates between lower and higher charge nuclei, at least in the range of Z shown for the α -process.

e-process This represents a high temperature process wherein thermodynamic equilibrium based on the relative nuclear binding energies is approached. Since ^{56}Fe has the lowest energy (most tightly bound) per nucleus, it has the highest abundance and the nuclei as a whole are called the iron peak elements.

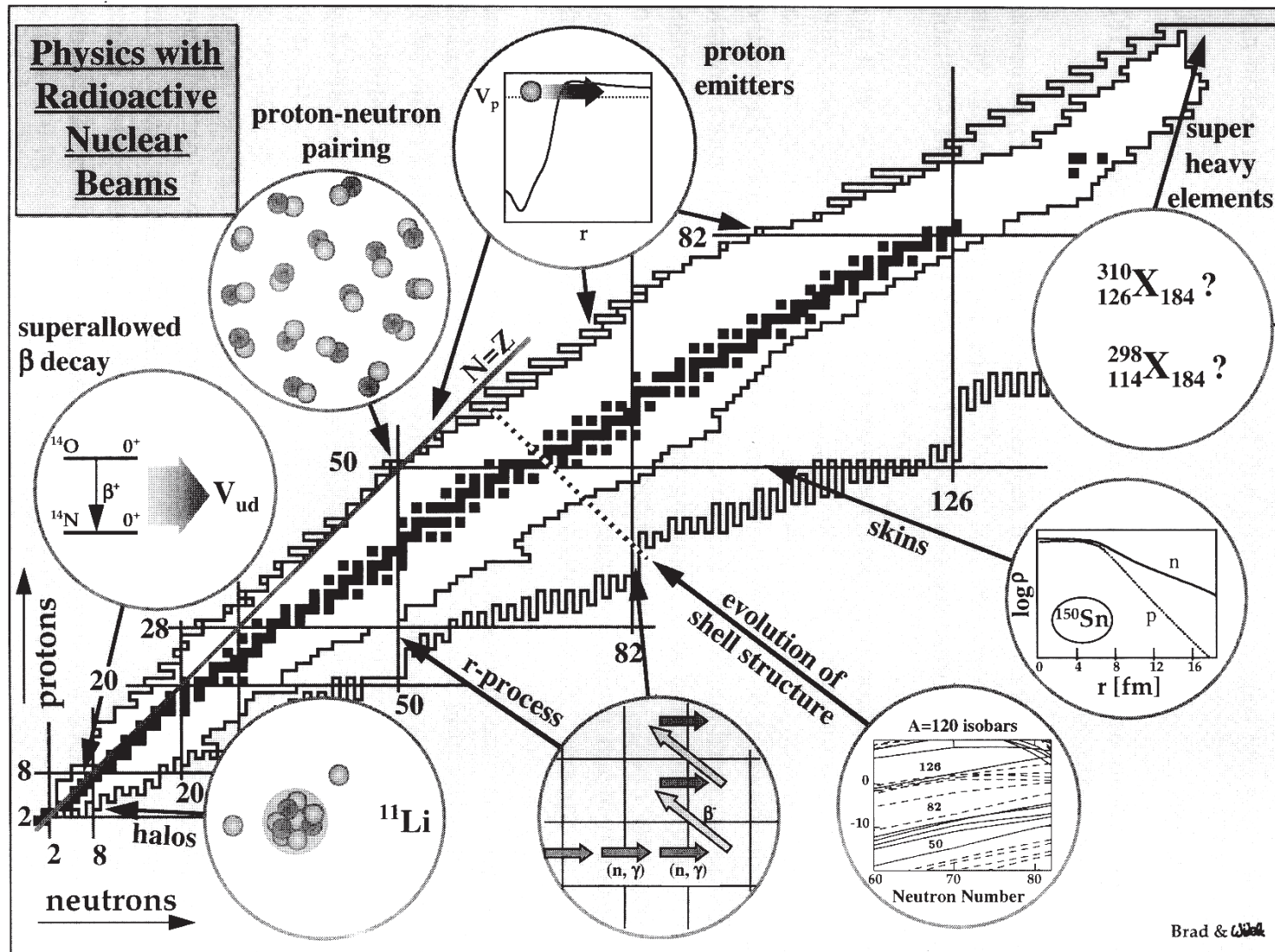
s-process These nuclei are formed by capture of neutrons onto iron-peak nuclei at a rate slow enough that a number of long-lived species (half-lives of hours to a few years) have time to decay between successive neutron captures. The site is generally believed to be thermally pulsing AGB stars.

r-process These nuclei are formed in events having a high neutron flux. The highest abundance species are those where highly unstable neutron-rich species with a closed neutron-shell are not able to capture an additional neutron during the event, then decay to a stable configuration after the event has ended. The process is believed to occur during supernovae.

The Principal Nucleosynthesis Processes as Summarized by B²FH



Paths of Nuclear Processes on the N - Z Plane



- The Dark squares indicate stable nuclei.
- The outlined area shows the boundary where either neutrons (on the right) or protons (on the left) drip out of the nucleus under laboratory conditions.
- The path of the r-process is shown. The s-process goes through the stable nuclei jumping the gaps or not depending on the half-life of the intermediate unstable species.
- The p-process is needed to produce species to the left of the s-process line.

The Major Stages of Nuclear Burning

Hydrogen Burning - Central

Most of the life of a star is spent burning hydrogen on the main sequence. Because of the relatively uniform structure of the main sequence star, the temperature gradient is not steep and the effects of hydrogen burning are spread over a large fraction of the stellar mass. Although the primary effect of hydrogen burning — the conversion of H to He — is concentrated toward the center of the star, other effects including the formation of ^3He and some CNO processing can alter abundances to mass fractions as large as $0.7M$.

The two principal ways of converting ^1H to ^4He are summarized on Figures 2 and 3 from Parker's article in "Physics of the Sun". These are attached. The relative importance of the two major processes ($p-p$ chain or CNO cycle) are shown in Figure 5-16 of Clayton's book. The temperature dependence of the $p-p$ chain is roughly T^4 while for the CNO cycle it is more like T^8 . The extra concentration towards the model center causes a convective core to form in the higher mass stars where the CNO cycle dominates the energy production.

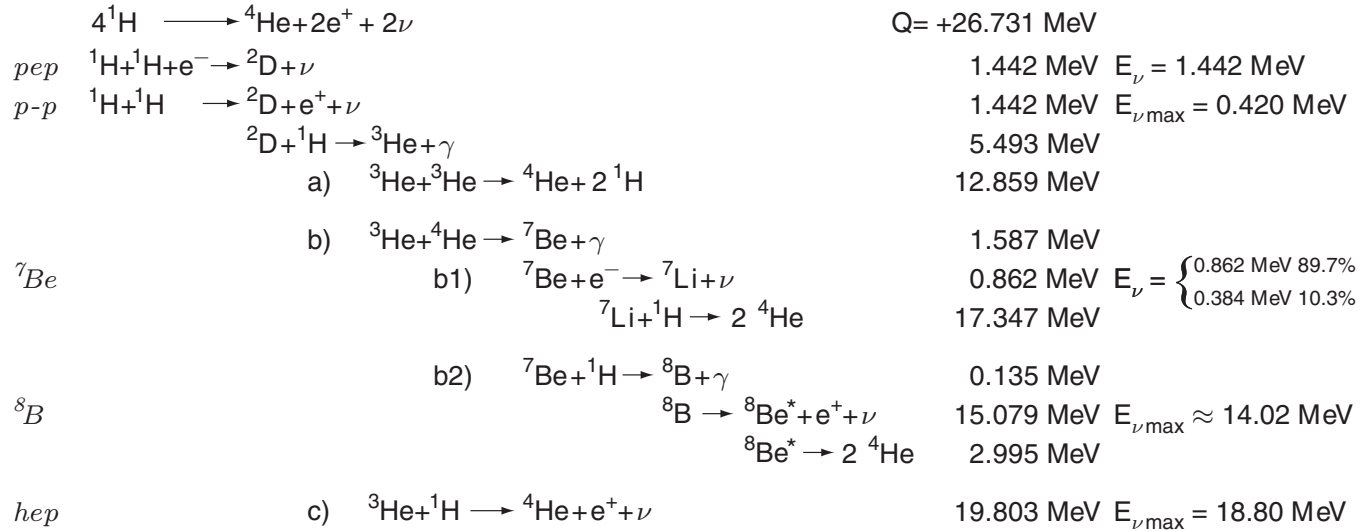
The abundance changes from the nuclear reactions include

- Destruction of ^2D .
- Formation of ^3He .
- Destruction of ^7Li , ^9Be and ^{11}B .
- Conversion of ^{12}C to ^{14}N .
- Conversion of ^{16}O to ^{14}N .

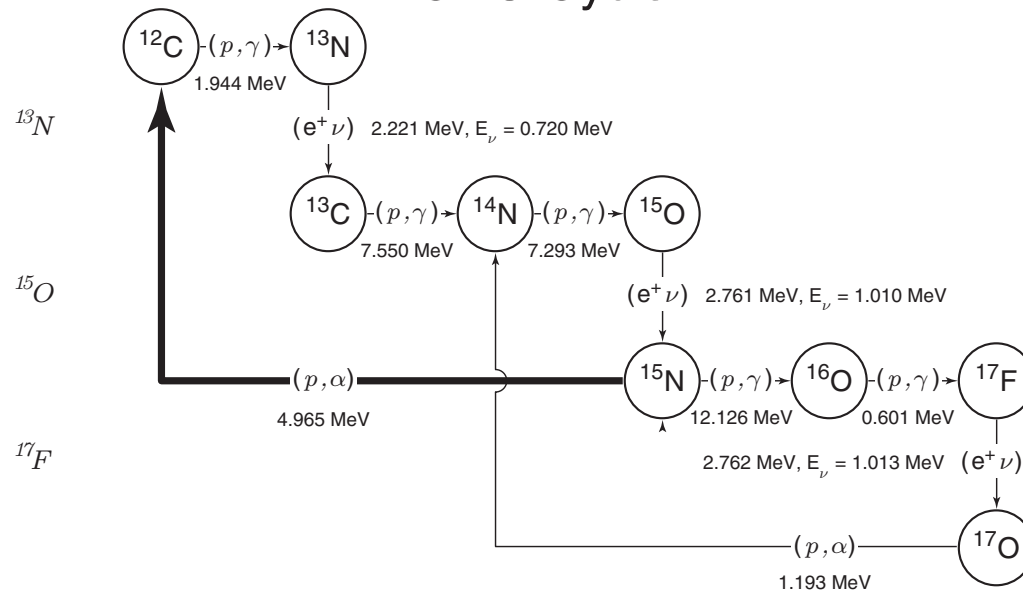
For the case of the sun, the details of the hydrogen burning are especially important because of the possibility of detecting the neutrinos from the nuclear reactions. The higher energy neutrinos are more easily detected so that the branching ratios between the three possibilities of the $p-p$ chain need to be known. The fact that the sun is static constrains the overall rate of energy production.

The Nuclear Reactions of Hydrogen Burning

p-p Chain



CNO Cycle



The Temperature Dependence of Reaction Rates

The number of reactions per second between nuclei X and a depends on the product of their densities in the gas $\rho X_X X_a$ where X_X is the mass fraction of X and X_a is the mass fraction of a . The temperature dependence comes from the fact that the reacting nuclei have energy due to the temperature of the gas. These thermonuclear reaction rates are governed by the competition between repulsive Coulomb barrier between like charged nuclei and the energy of nuclei with much more than the typical kT per particle. This is described as being on the tail of the thermal distribution. The barrier penetration factor produces a strong dependence on the product of the two nuclear charges $Z_X Z_a$ while the kinetic energy factor produces a dependence on the reduced mass of the pair $A = m_X m_a / (m_X + m_a)$. The rate then has a factor including the following:

$$R_{aX} \propto \exp \left[-42.48 \left(\frac{Z_X^2 Z_a^2 A}{T_6} \right)^{1/3} \right]. \quad (39)$$

The most abundant particles initially are the protons and the factors in the exponential are most favorable for these two to react. However, there is no stable ${}^2\text{He}$ nucleus so the product of the two protons has to be ${}^2\text{D}$. This requires the conversion of one proton to a neutron along with a neutrino so that the reaction involves the weak interaction. Consequently, the rate of the reaction is smaller than for a typical strong interaction reaction by the ratio of the coupling constants. The coupling constants are roughly in the ratios:

Force	Relative Strength
Pion-nucleon (strong force) strength	1.0
Electromagnetic strength	1/137
Weak (beta-decay) coupling strength	10^{-5}
Gravitational Coupling strength	10^{-39}

Consequently, the proton-proton reaction is disfavored by a factor of roughly 10^5 . To make up for this factor the temperature for hydrogen burning is about 18 times higher than would otherwise be the case. This causes the main sequence to come at a radius like that of the sun instead of about 18 times larger.

Details of Hydrogen Burning

The equations giving nuclear abundance changes often have the form:



and sometimes there will be a further step where Y decays to Z as in:



so that the net result is to produce Z instead of Y when a and X react. Additionally there might be still another reaction producing X :



Based on these reaction sequences we might write the following equations:

$$\frac{1}{A_X} \frac{dX_X}{dt} = R_{cW} X_W X_c - R_{aX} X_X X_a \quad (43)$$

$$\frac{1}{A_Y} \frac{dX_Y}{dt} = R_{aX} X_X X_a - R_Y X_Y \quad (44)$$

$$\frac{1}{A_Z} \frac{dX_Z}{dt} = R_Y X_Y . \quad (45)$$

Often the intermediate species Y has a low abundance and does not represent a place where a significant number of nuclei are stored during the burning process. In this case we can consider these species to have a steady state abundance and set $\frac{dX_Y}{dt} = 0$. This then lets us write:

$$R_Y X_Y = R_{aX} X_X X_a \quad (46)$$

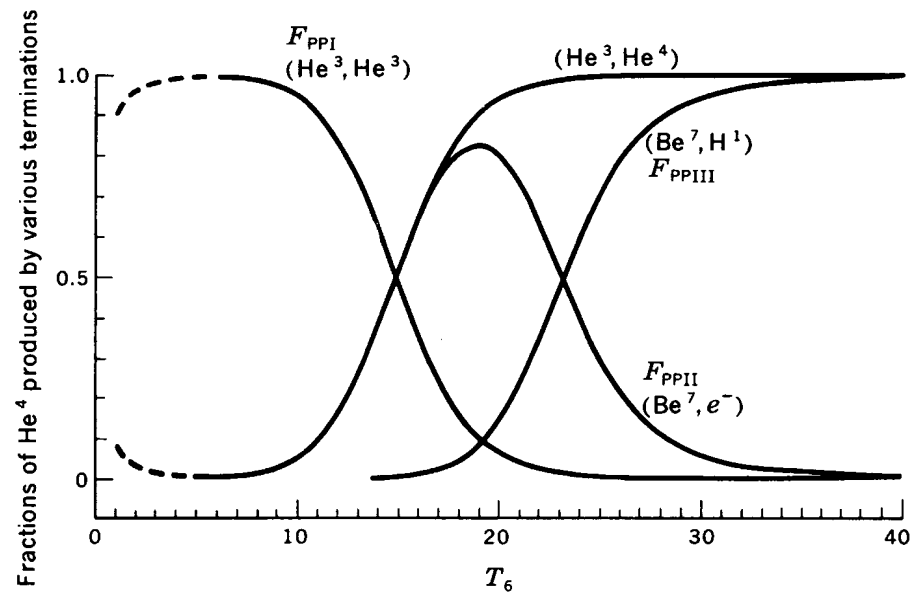
so that:

$$\frac{1}{A_Z} \frac{dX_Z}{dt} = R_{aX} X_X X_a \quad (47)$$

and as far as the calculation of the evolution of X_Z is concerned, the intermediate species does not play a role.

Balance in the $p - p$ Chain

Since the $p - p$ reaction is the last one to remain at low temperatures, the sequence stops at ${}^3\text{He}$. At higher temperatures the ${}^3\text{He}$ can be burned by either ${}^3\text{He}$ or ${}^4\text{He}$. Both reactants have the same charge factor but the second option (sequence b) has a higher A of $4 \times 3 / (4 + 3) = 1.714$ instead of $3 \times 3 / (3 + 3) = 1.5$. This means that the b) termination is favored at higher temperatures. In addition, the b1 termination is largely independent of temperature (a slight decrease in rate at higher temperatures due to phase space factors for the free electron) while the b2 termination is strongly temperature dependent since it is a charged particle reaction. The combination of these factors yields the pattern below:



In this representation the notation I is the same as branch a), II is branch b1) and III is branch b2).

The steady state abundance of ${}^2\text{D}$ relative to ${}^1\text{H}$ is of order a few times 10^{-18} so that once hydrogen burning has begun the primordial Deuterium is quickly removed. In contrast the steady state abundance of ${}^3\text{He}$ is high at low temperatures and can reach a mass fraction of 0.001 or more. The termination through capture of a proton by ${}^3\text{He}$ is extremely rare and plays no role except for the production of the highest energy neutrinos from the sun.

Approach to Steady State in the CNO Cycle

For equations of the type of equation 75, the species in the middle, X_Y approaches the value X_Y^{ss} which gives zero on the right:

$$X_Y^{ss} = \frac{R_{aX} X_X X_a}{R_Y} \quad (48)$$

If the source abundances X_X and X_a are constant then the intermediate abundance has a time dependence of the form:

$$X_Y = X_Y^0 e^{-t/\tau_Y} + X_Y^{ss} (1 - e^{-t/\tau_Y}) \quad (49)$$

$$\text{where } \tau_Y = \frac{1}{A_Y R_Y} . \quad (50)$$

The CNO cycle has several parts which have the character of the above system. As an illustration consider the following model:



As a general rule, we can drop out the ^{13}N and the ^{15}O as being in steady state at all times. The ^{13}C is a special case. It is often in steady state but because it winds up with a high abundance and is also observable in various molecular lines, it is worth keeping in explicitly. As a simplification of notation, I use the atomic weight as the tag denoting the species. The equations are then:

$$\frac{1}{12} \frac{dX_{12}}{dt} = R_{1,14} X_1 X_{14} - R_{1,12} X_1 X_{12} \quad (56)$$

$$\frac{1}{13} \frac{dX_{13}}{dt} = R_{1,12} X_1 X_{12} - R_{1,13} X_1 X_{13} \quad (57)$$

$$\frac{1}{14} \frac{dX_{14}}{dt} = R_{1,13} X_1 X_{13} - R_{1,14} X_1 X_{14} \quad (58)$$

The CNO Cycle (cont.)

The atomic weight factors on the left of each of the equations are needed because the right hand sides give the number of reactions whereas the left hand side has to give the change in the mass fraction. Since the product is heavier than the heavier reactant, each reaction reduces the mass fraction of the reactant less than it increases the mass fraction of the product. An alternate way of setting up these systems is to use another variable $Y_X = X_X/A_X$. The R factors then need to include appropriate products of atomic weights but are otherwise the same as already set up.

We can define a series of species lifetimes and species steady state abundances:

$$\tau_{12} = \frac{1}{12} R_{1,12} X_1 \quad (59)$$

$$\tau_{13} = \frac{1}{13} R_{1,13} X_1 \quad (60)$$

$$\tau_{14} = \frac{1}{14} R_{1,14} X_1 \quad (61)$$

and

$$\frac{X_{12}^{ss}}{X_{13}^{ss}} = \frac{R_{1,13}}{R_{1,12}} \quad (62)$$

$$\frac{X_{13}^{ss}}{X_{14}^{ss}} = \frac{R_{1,14}}{R_{1,13}} \quad (63)$$

$$\frac{X_{14}^{ss}}{X_{12}^{ss}} = \frac{R_{1,12}}{R_{1,14}} \quad (64)$$

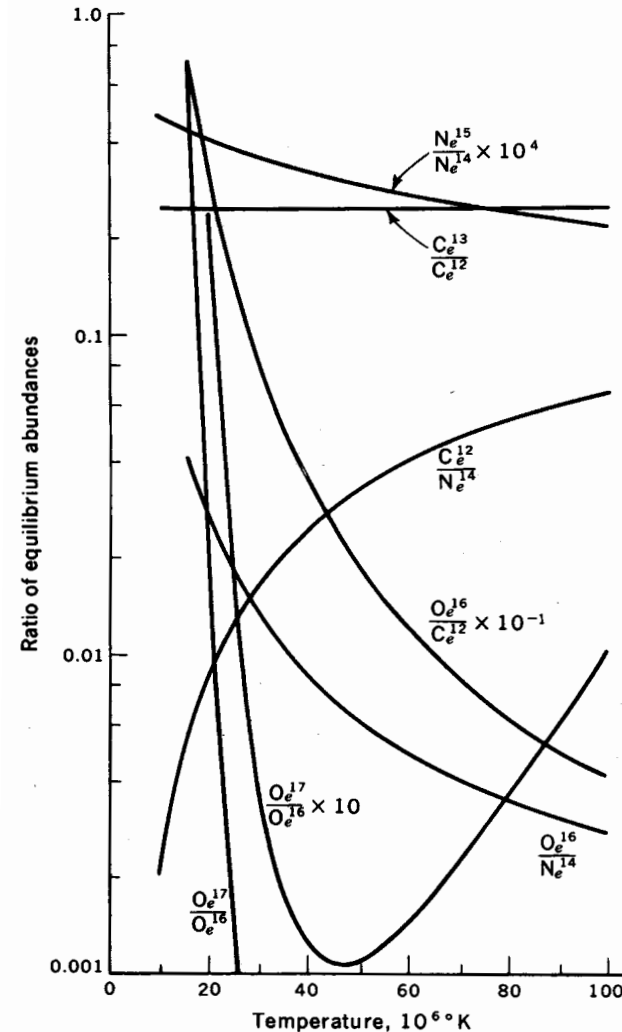
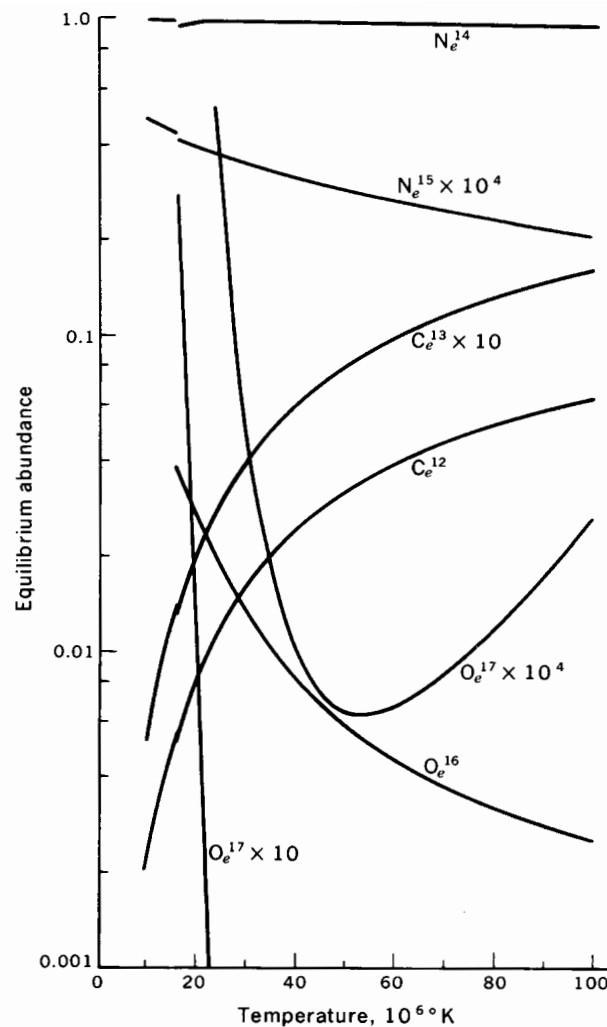
You will notice that the last three equations are not independent since the third can be derived from the ratio of the first two. Therefore a third equation is required and that is:

$$\frac{X_{12}}{12} + \frac{X_{13}}{13} + \frac{X_{14}}{14} = \frac{X_{12}^0}{12} + \frac{X_{13}^0}{13} + \frac{X_{14}^0}{14} \quad (65)$$

CNO Cycle Approach to Steady State

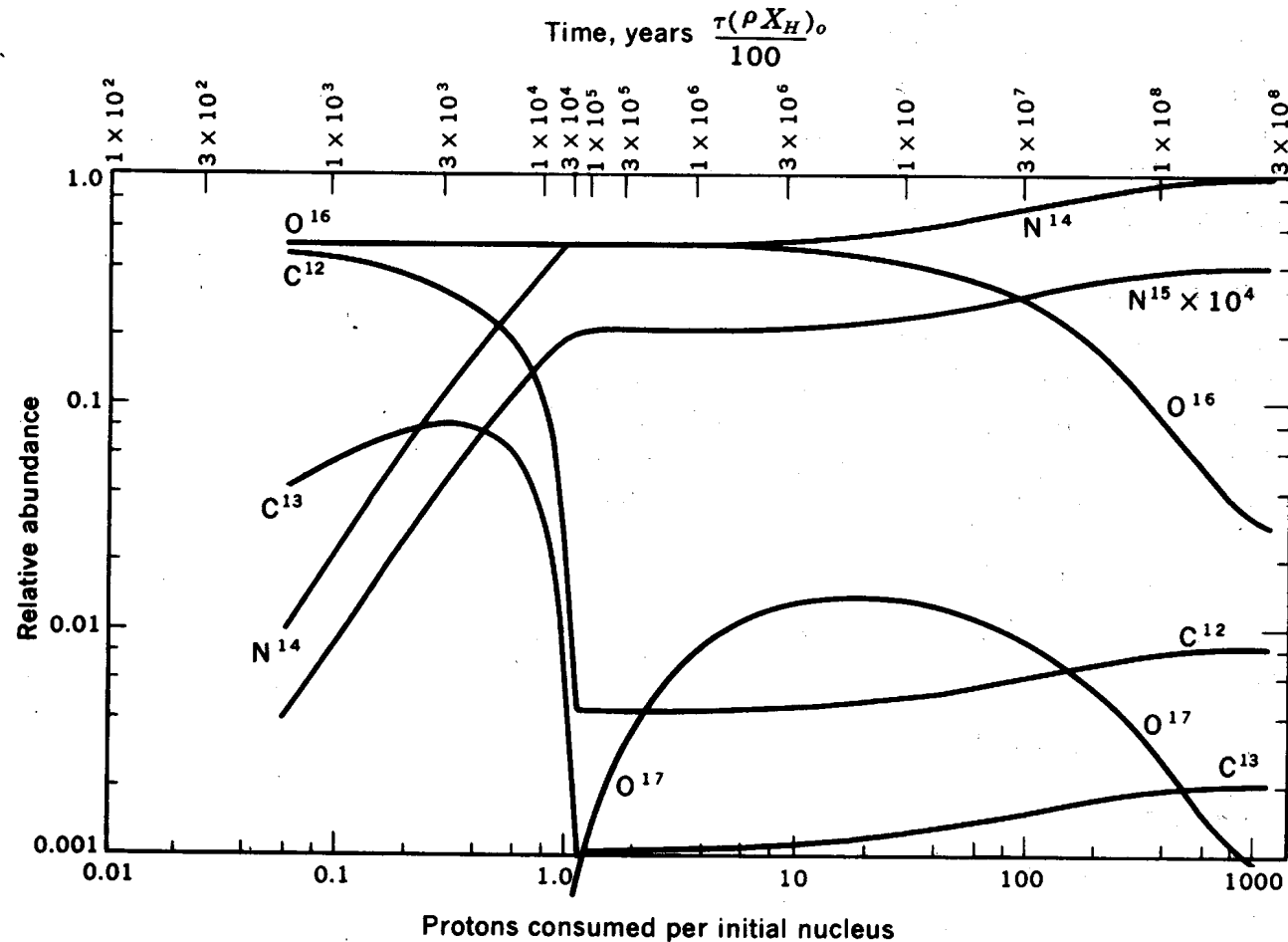
The system of equations can be solved in a straight-forward manner in terms of eigenfunctions which diagonalize the resulting matrix equation. Each sub-part of the system approaches its local steady state at a rate which is governed by the dominant terms.

The following two figures give the dependence of the full set of CNO abundances on temperature. These figures are based on somewhat older reaction rates and should be revised to more modern data in the event that the results are important.



CNO Cycle Approach to Steady State (results)

The abundance equations can be integrated analytically or numerically. The parameter giving the approach to steady state is essentially the amount of hydrogen consumed divided by the total initial abundance of the CNO elements. This parameter gives four times the effective number of times the cycle has been traversed since each time around the loop four hydrogen nuclei are consumed. For a Pop I star this number has to be of order 50 to use up the hydrogen whereas for a Pop II star it must be between 500 and 5000 depending on the degree to which the heavy elements are underabundant. A sample approach to steady state is given below:



Hydrogen Burning in a Shell Source

After the depletion of hydrogen in the stellar core, nuclear energy can no longer be generated from the center of the star. The lack of energy to be transported from the stellar center causes the temperature gradient to decrease and an isothermal core starts to form. For the lower mass stars which did not have a convective core, this change is gradual and the shell source forms smoothly as the central hydrogen runs out. For the higher mass stars the situation is a bit different because the presence of mixing holds up the central hydrogen abundance longer than would otherwise be possible. Also, because the energy generation rate depends on only the first power of the hydrogen abundance, as long as a small amount of hydrogen is present, a slight increase in temperature is all that is required to maintain the generation of enough energy to sustain the convective core. Typically the convective core will persist until only a very small mass fraction of hydrogen remains in the convective core and then convection abruptly stops when the hydrogen abundance actually becomes zero. The transition from the adiabatic temperature gradient (polytropic index $3/2$) to a nearly isothermal structure causes an abrupt shrinking of the star and produces a kink in the isochrones on the H.-R. diagram.

After the depleted core has formed and started to become isothermal, another factor comes into play. The isothermal case of the polytropic configuration can be analyzed analytically. It turns out that to fit together an isothermal core surrounded by a polytrope of index 3, no configuration can be found when the mass of the core is above about $0.12 \times M$. This conclusion applies when the gas is non-degenerate. When the depleted core exceeds this limit, it must contract and both develop degenerate electron pressure support and cease to be isothermal. The onset of core contraction due to this limit corresponds to the transition from thick shell source burning to thin shell source burning. Because of the high temperature exponent involved in the nuclear rates, the zone of energy generation is about one or two pressure scale heights. The mass of this zone is:

$$\frac{1}{\Delta M_{SS}} = \frac{1}{P} \frac{dP}{dM_r} = -\frac{GM_r}{4\pi r^4 P}$$

so that:

$$\Delta M_{SS} \propto \frac{r^4 \rho T}{M_{core}}$$

The core contraction decreases r so the ΔM_{core} decreases.

Expansion to the Red Giant Phase — The Mirror Effect

As the core contracts, it initially can be thought of as including the hydrogen rich material. The nuclear energy generation rate of the CNO cycle has the form:

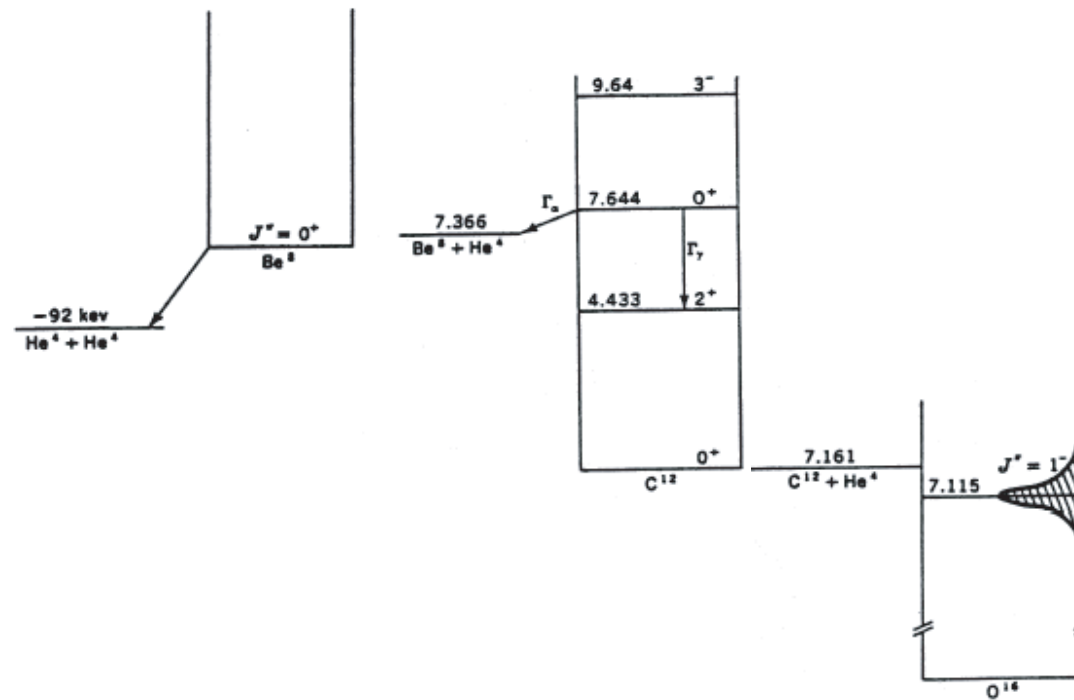
$$\epsilon_{CNO} = \epsilon_0 X_H X_{CNO} \rho T^{-\frac{2}{3}} \exp\left(-\left(\frac{152.3}{T_6}\right)^{2/3}\right) f_{CNO}$$

where ϵ_0 is a constant equal to approximately 7×10^{27} ergs/gm/sec. The logarithmic derivative of ϵ_{CNO} gives the effective temperature exponent of the energy generation:

$$\nu = \frac{T}{\epsilon_{CNO}} \frac{\partial \epsilon_{CNO}}{\partial T} = \frac{1}{3} \left(\frac{152.3}{T_6} - 2 \right)$$

which at a typical post-main sequence central temperature of $T_6 = 30$ to 60 yields $\nu = 15.7$ to 12.3 . This very steep temperature dependence means that the onset of hydrogen burning is very abrupt. One can require approximately that the product of ϵ_{CNO} and ΔM_{ss} is roughly equal to the star luminosity. This places a very stiff requirement on the temperature of the shell source. If the shell source temperature exceeds that value, the shell will produce excess luminosity that can not be transmitted through the outer envelope. The untransmitted luminosity is absorbed in the outer envelope and causes the envelope to expand. The envelope expansion crosses over the core contraction in just the right way to keep the shell source temperature constant. When the contracting core ignites a new energy source like He burning, the argument goes in reverse as long as the hydrogen shell source is providing the bulk of the star's luminosity. In this way the shell source acts like a fulcrum in a lever and the overall result is called the mirror effect.

Helium Burning - The 3- α process



- The first step of the 3- α process is the transient combination of two ${}^4\text{He}$ nuclei into an unstable ${}^8\text{Be}^*$ nucleus. This nucleus is energetically disfavored but nonetheless is created with an equilibrium abundance which is very low. According to the Saha Equation applied to the nuclei this species abundance is:

$$N({}^8\text{Be}) = N_{{}^4\text{He}}^2 \omega f \frac{h^2}{(2\pi\mu kT)^{3/2}} \exp(-E_{r, {}^8\text{Be}}/kT) \approx 1.87 \times 10^{-33} N_{{}^4\text{He}}^2 f T_8^{-3/2} 10^{-4.64/T_8} \quad (66)$$

where f is an electron screening correction factor (not too far from unity).

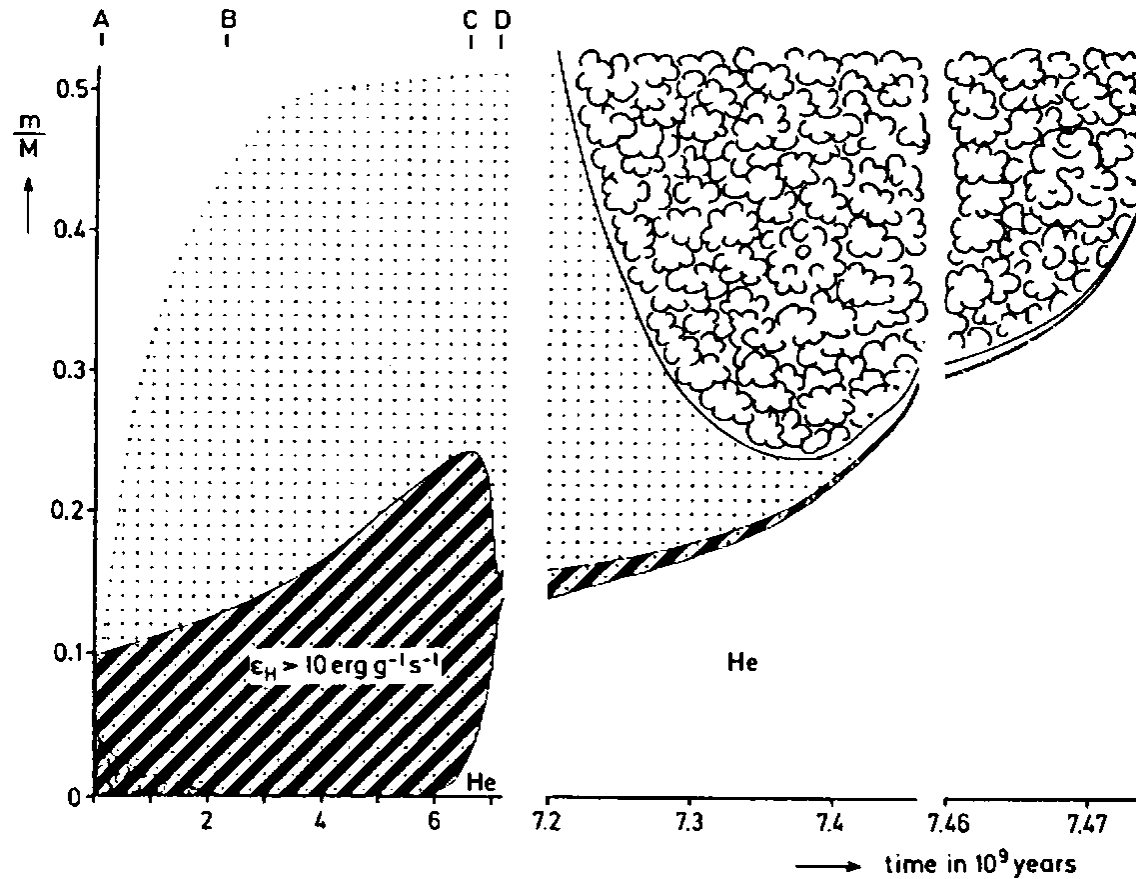
- After the ${}^8\text{Be}^*$ nucleus is formed, it can further combine with another α particle again according to the Saha Equation:

$$N_{12\text{C}^*} = N({}^8\text{Be}^*) N_{{}^4\text{He}} f \frac{h^2}{(2\pi\mu kT)^{3/2}} \exp(-E_{r, 12\text{C}}/kT) \quad (67)$$

so that

$$r_{3\alpha \rightarrow 12\text{C}} = 9.8 \times 10^{-54} \frac{N_{{}^4\text{He}}^3}{T_8^3} f \exp\left(-\frac{42.94}{T_8}\right) \text{ cm}^{-3} \text{ s}^{-1} \quad (68)$$

Evolution up to the He Core Flash



The sequence of events leading up to the helium core flash is shown above as a function of time. The dotted areas are where there is a gradient of the hydrogen/helium ratio. The bubbly areas are convective and the cross-hatched areas are where the H to He burning rate exceeds a critical value.

Helium Ignition

The contraction of the core of the star with a helium shell source is largely driven by the addition of mass. As we saw in the discussion of the white dwarf, as the mass of the degenerate region becomes larger, the radius decreases and the density increases. This causes a regular decrease in the mass in the hydrogen burning shell and a consequent regular increase in the temperature. The shell source is generally non-degenerate so that there remains some compression and temperature increase between the shell and the degenerate core. The gradual increase in shell source temperature plus the compressional temperature rise eventually causes the depleted core temperature to become high enough to ignite the Helium. Due to neutrino losses at the highest densities in the center of the core, the temperature there is lower than at a point a bit further out. The temperature is inverted and energy is conducted inwards to the center where it is lost to the neutrino emission processes. At the point of peak temperature the ignition of the helium begins under conditions of great degeneracy with the non-degenerate pressure due to the nuclei and the pressure due to the high energy electrons providing only a percent or two of the total pressure. Consequently, the initial temperature rise from the ignition of the new fuel does not cause a significant increase in the pressure so that the process begins as a runaway. Recall that the condition for adiabatic decompression is the same as the condition for the degeneracy to be constant. Consequently, as the temperature rises to lift the degeneracy, it also becomes superadiabatic and generates convective motions. These motions allow the energy released from the new nuclear fuel to be distributed over a larger mass shell and decreases the rate of temperature rise since the peak energy generation remains at the point of highest temperature. The extra mass which is heated by the convection causes the effective heat capacity of the zone to increase. Since the rate of temperature rise is

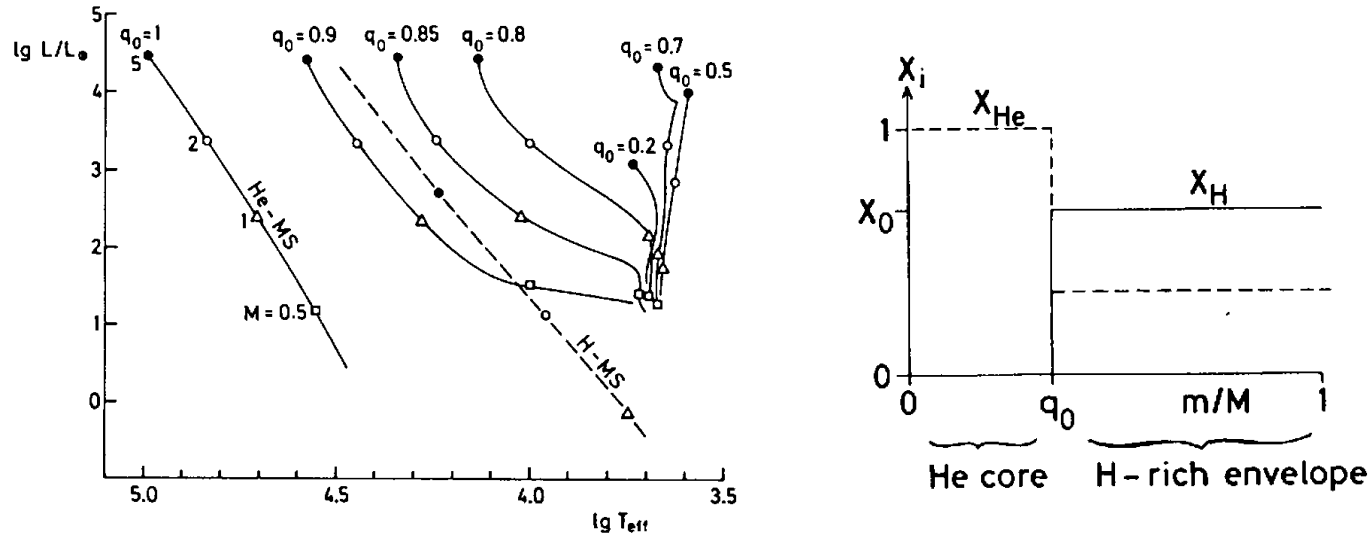
$$\int T \frac{dS}{dt} dM_r \approx \int C_P \frac{dT}{dt} dM_r = \int \epsilon_{\text{NUC}} dM_r \quad (69)$$

so that

$$\tau = \left(\frac{d \ln T}{dt} \right)^{-1} \approx \frac{\int T C_P dM_r}{\int \epsilon_{\text{NUC}} dM_r} \quad (70)$$

More on the Helium Ignition Flash

The rate of growth of the temperature during the flash increases as the value of ϵ_{nuc} grows. The dilutive effect of the convective process dampens the growth and the time scale never becomes comparable to the sound travel time which is of order $\delta l / c_{\text{sound}} = \frac{10^8 \text{ cm/s}}{10^8 \text{ cm}} = 1 \text{ sec}$. The actual growth times in integrations done by the Kippenhahn group and by Schwarzschild and Härm are at a minimum of about 0.1 day so the critical conditions are not reached. Should the effect of convection be left out, the mass spreading effect in slowing down the growth would not be available and the process would become an unbounded runaway. There have been calculations which result in the disruption of the star from this flash when convection is turned off.

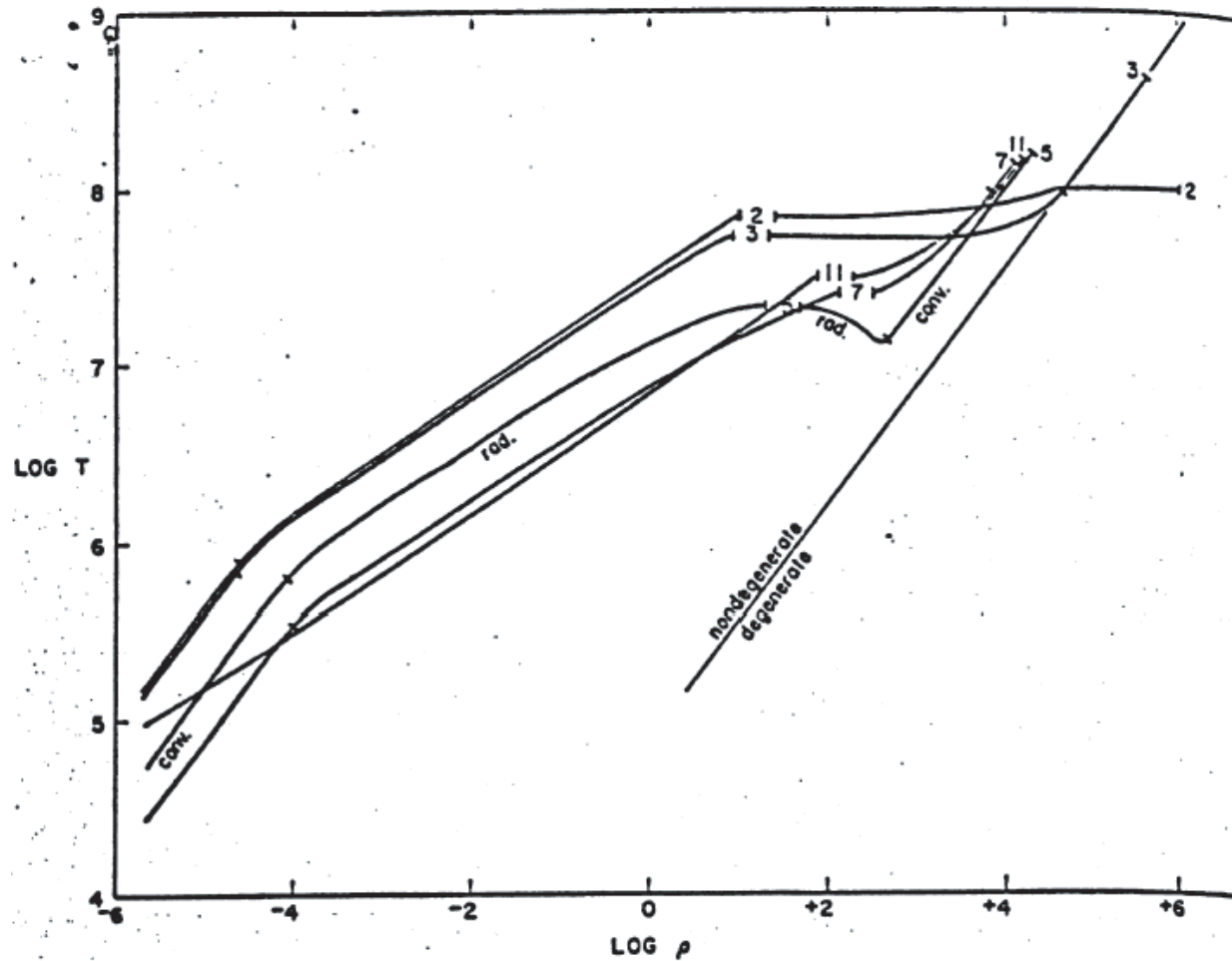


The result of the Helium flash can be understood in terms of a generalized main sequence type calculation in which the gravitational and thermal change terms are dropped. The nuclear abundance distribution is shown on the right and the resulting position on the horizontal branch is shown on the left.

Following the readjustment of the star from the helium flash, the non-degenerate core shifts its peak temperature to the center and begins a core helium burning with a hydrogen shell. These stars form a knot near the convective track for Pop. I stars and form the horizontal branch for Pop. II stars.

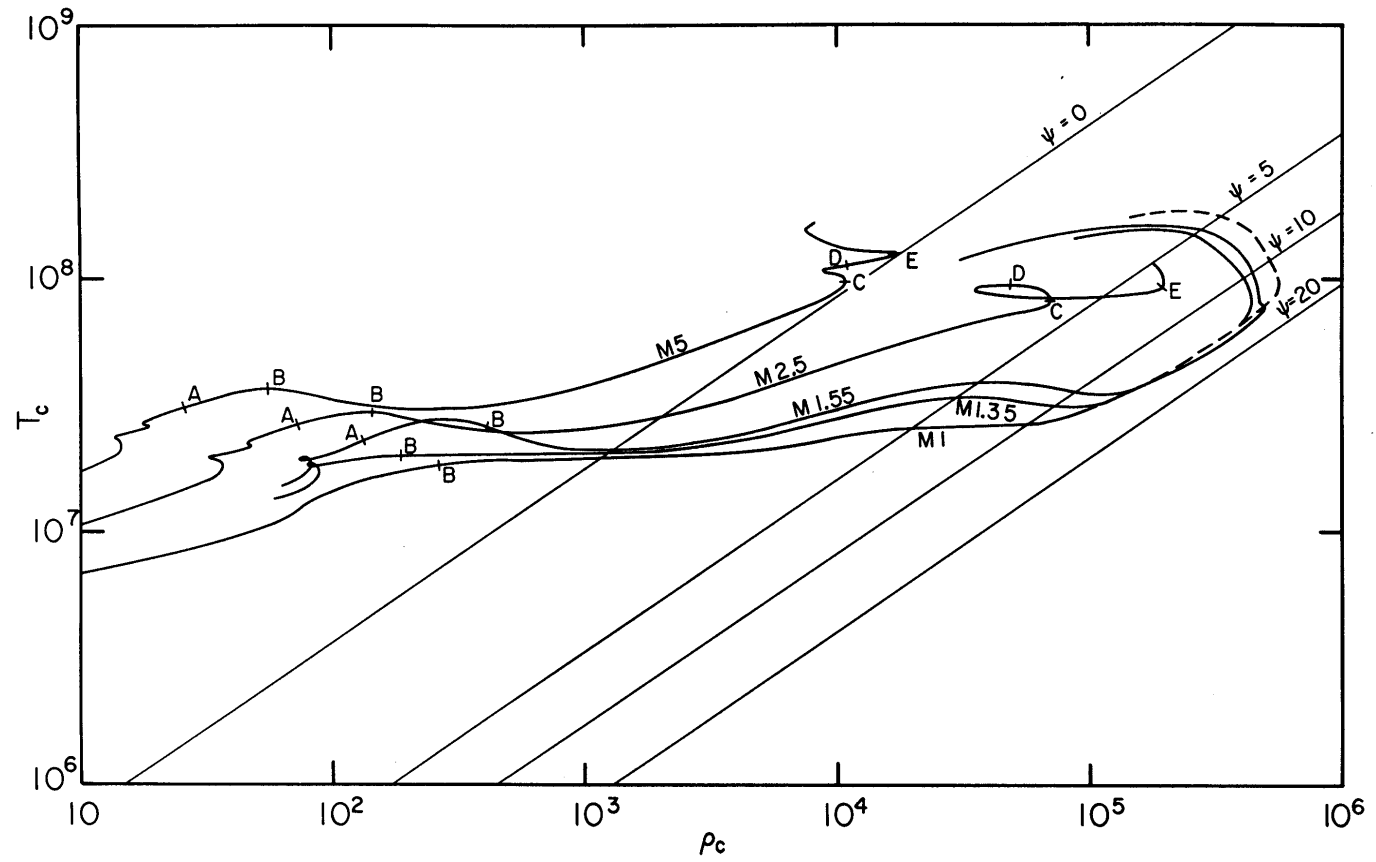
Helium Ignition Flash

This event was discovered by Schwarzschild and Härm. Without neutrino losses it happens at the center of the contracting white-dwarf-like configuration. A sequence of $\log(\rho) - \log(T)$ profiles are given below:

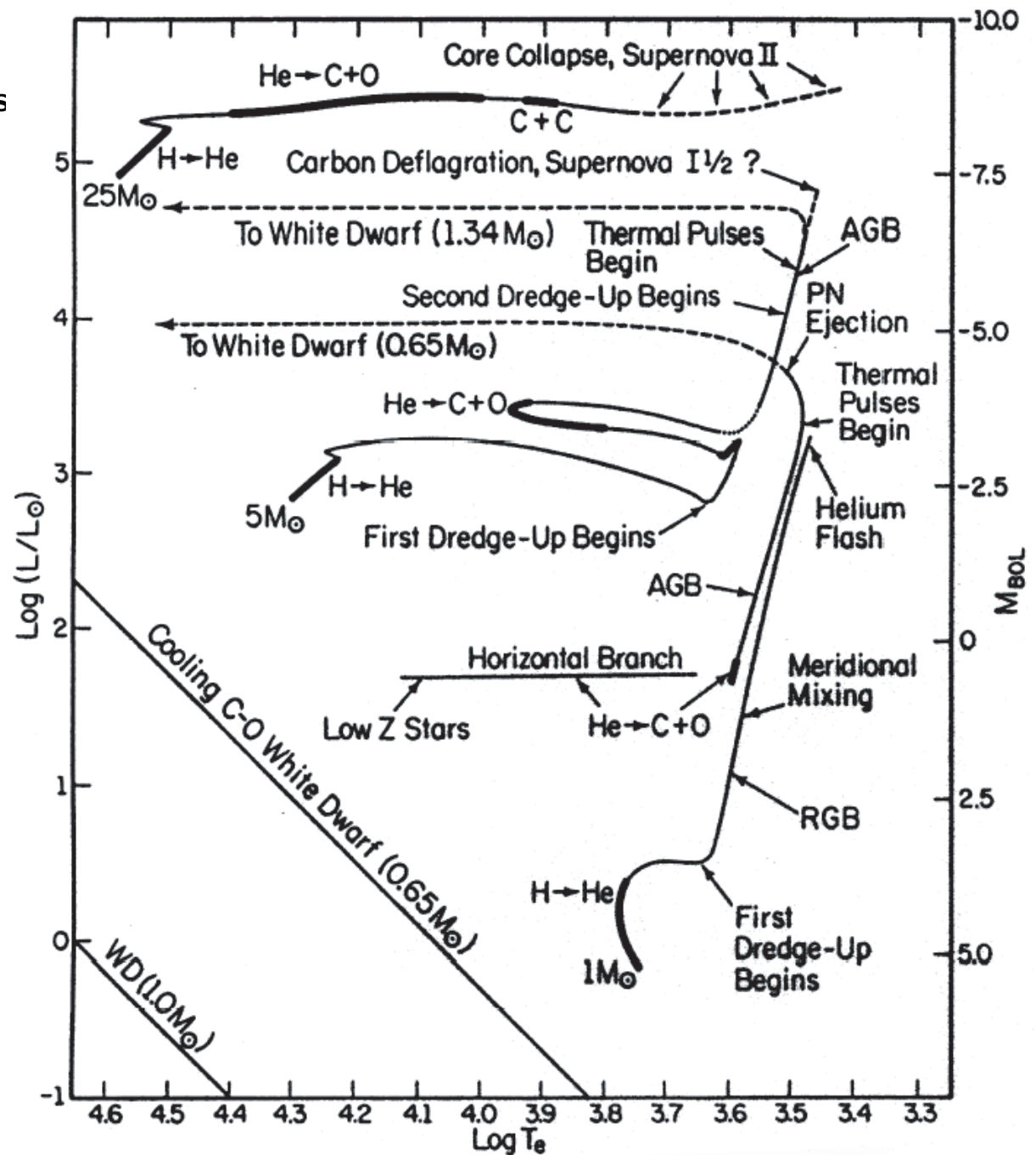


As the energy from the reaction is released, the temperature rises. Initially the pressure does not respond because the gas is supported by electron degeneracy alone. When the degeneracy is lifted then the star begins to expand and undergoes a reverse mirror-effect change.

Central temperature and density evolution



Context of nuclear evolution events



I. Iben Jr. and A. Renzini (eds.), *Physical Processes in Red Giants*, 3-24. Copyright © 1981 by D. Reidel Publishing Company.

Shell Source Structure

Let us go back and look at the structure equations following a development done by Paczynski (1970AcA....20..287P). Using the energy transport equation and the equation of hydrostatic equilibrium we have:

$$\frac{dT}{dM_r} = -\frac{1}{16\pi^2 r^4} \frac{3\kappa_{\text{Ross.}}}{16\sigma T^3} L_r = -\frac{1}{16\pi^2 r^4} \frac{3\kappa_{\text{Ross.}}}{ac(dT^4/dT)} L_r \quad (71)$$

and

$$\frac{dP}{dM_r} = -\frac{GM_r}{4\pi r^4} \quad (72)$$

Where I have used $\sigma = ac/4$. After combining the terms in temperature in the first of these and taking the ratio of them we get:

$$\frac{d(aT^4/3)}{dP} = \frac{\kappa_{\text{Ross.}} L_r}{4\pi Gc M_r} \quad (73)$$

Under conditions outside a shell source the opacity is largely electron scattering $\kappa_{\text{Ross.}} = 0.2(1 + X)\text{cm}^2/\text{gm}$, the mass above the shell source is constant until you get into the convective envelope and the luminosity is constant also until you get into the convective envelope. This means that the right hand side of the above equation is a constant and that the solution can be found immediately by integration:

$$aT^4/3 = \frac{\kappa_{\text{Ross.}} L_r}{4\pi Gc M_r} P + C_1 . \quad (74)$$

As long as the ratio of pressure and temperature near the base of the convection zone to the values just outside the shell source is very small, we can assume the value of the constant of integration C is zero. Also using the fact that the radiation pressure is $aT^4/3$ and taking $1 - \beta = P_{\text{rad}}/P$ we get:

$$1 - \beta = \frac{aT^4/3}{P} = \frac{\kappa_{\text{Ross.}} L_r}{4\pi Gc M_r} = \text{a constant.} \quad (75)$$

It is worth noting that $1 - \beta$ is just the ratio of the actual luminosity to the Eddington Luminosity:

$$L_{\text{Eddington}} = \frac{4\pi Gc}{\kappa_{\text{Ross.}}} M_r \quad (76)$$

Shell Source Structure (cont.)

We may rewrite the radiative diffusion equation with r as the independent variable instead of M_r at which point the constant ratio of P to T^4 allows a solution for T as a function of r . The diffusion equation in this form is:

$$\frac{dT}{dr} = -\frac{3\kappa_{\text{Ross.}\rho} L_r}{16\pi acT^3 r^2} = \frac{\kappa_{\text{Ross.}\rho T}{16\pi c(aT^4/3)} \frac{L_r}{r^2} \quad (77)$$

After using $\beta P = \rho R T / \mu$ and $(1 - \beta)P = aT^4/3$ then using equation (75) we get:

$$\frac{dT}{dr} = -\frac{\mu \kappa_{\text{Ross.}} L_r}{R 16\pi cr^2} \frac{\beta}{1 - \beta} = -\frac{\mu \kappa_{\text{Ross.}} L_r}{R 16\pi cr^2} \frac{\beta}{((\kappa_{\text{Ross.}} L_r)/(4\pi GcM_r))} = -\frac{\mu}{4R} \frac{GM_r}{r^2} \beta \quad (78)$$

Now since we know from above that β is constant and because M_r in the zone above the shell source is essentially constant – the shell source has a very small mass – we can integrate the above in r to obtain:

$$T = \frac{\mu}{4R} \frac{GM_r}{r} \beta + C_2 \approx \frac{\mu}{4R} \frac{GM_r}{r} \beta \quad (79)$$

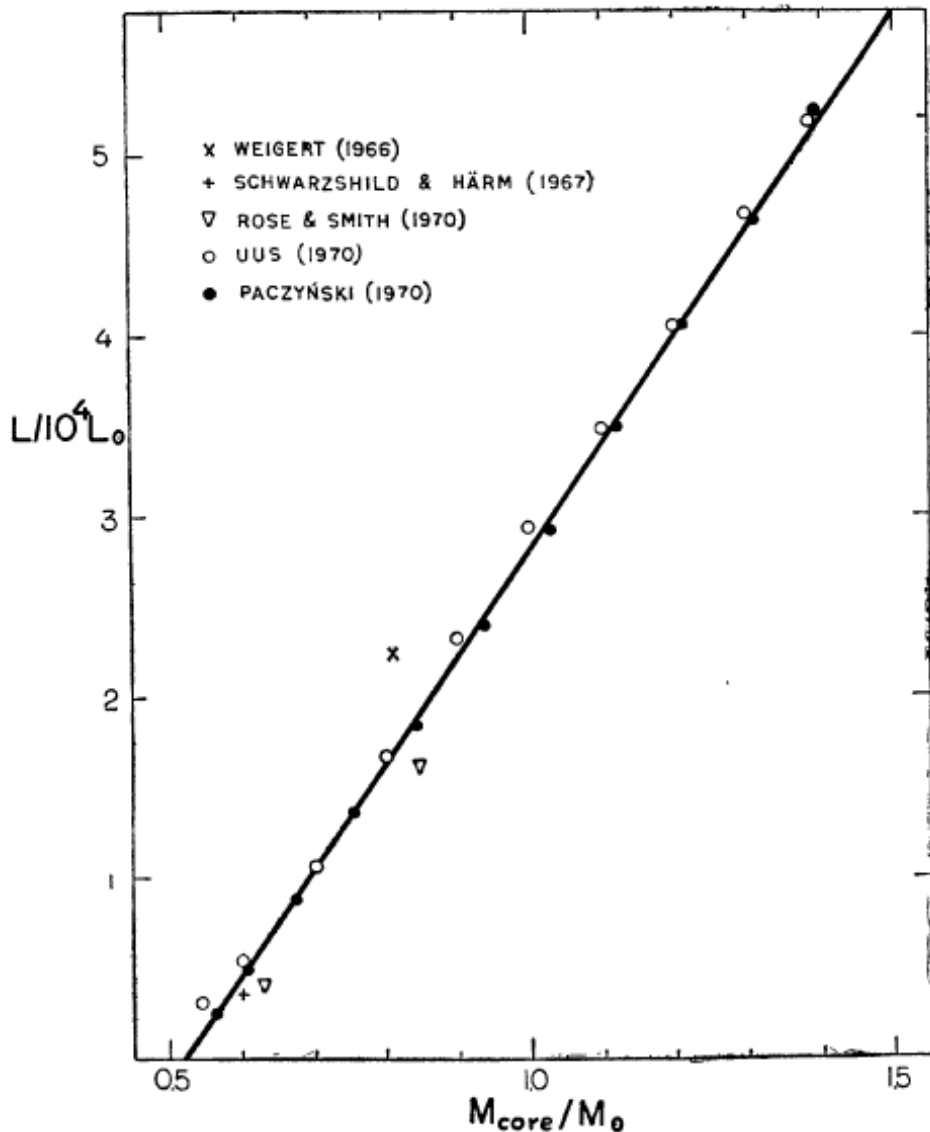
where C_2 is another constant of integration which is very close to zero since the temperature of the shell source is many times larger (~ 100) than the temperature at the base of the convective envelope. Let us designate the radius, mass, luminosity and Eddington luminosity measured in solar units through the addition of a superscript tilde: $L_r/L_\odot = \tilde{L}_r$, etc. Using this notation we have numerically:

$$\tilde{L}_{\text{Eddington}} = \frac{64780}{1 + X} \tilde{M}_r \quad (80)$$

$$\tilde{L}_r = (1 - \beta) \tilde{L}_{\text{Eddington}} \quad (81)$$

and at $T = 10^7 \text{K}$ we get for the mass and density:

$$\rho = 0.0306 \frac{\beta}{1 - \beta} \mu \quad \text{and} \quad \tilde{r} = 0.578 \tilde{M}_r \beta \mu \quad (82)$$



The Core Mass – Core Luminosity Relation

Paczynski(1971AcA....21..417P) carried out and summarized a number of calculated results for the region outside shell sources with core masses covering a range of values. He found that the computed results are well fitted by the following equation:

$$\tilde{L}_{\text{shell source}} = 59250(\tilde{M}_{\text{core}} - 0.522) \quad (83)$$

The fit of the calculated shell source luminosity (i.e. the luminosity produced by the shell source and measured outside the energy producing layers) to the core mass is shown in the figure to the left.

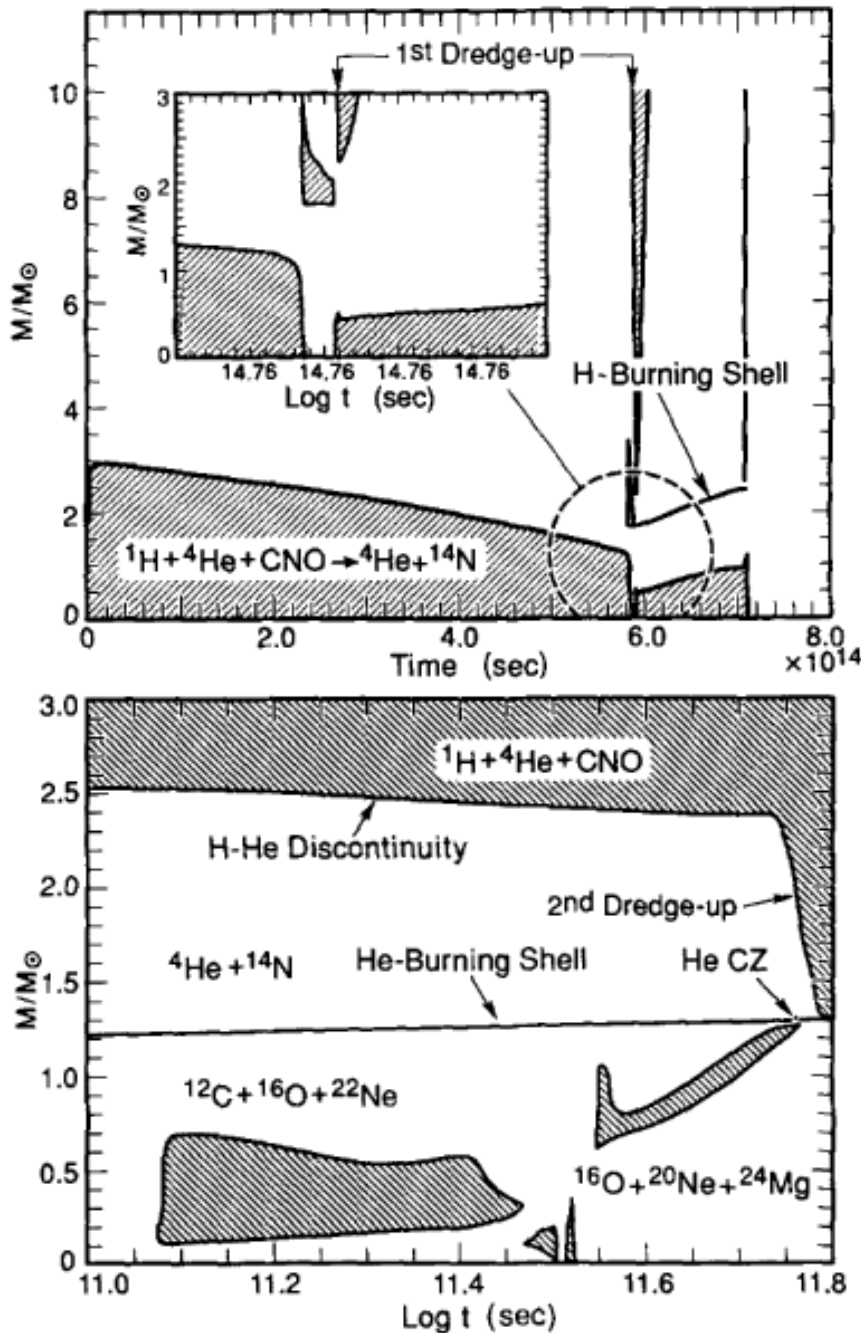
Although the cause for the good correlation is not fully explained, the close relationship to the Eddington limit luminosity makes it clear that the conditions in the region between the shell source and the base of the convective envelope naturally adjust so that this region has a low but not vanishing density. In this case, β is less than unity but not much less than 0.1. That makes the electron scattering opacity dominant. As the core mass grows, the star luminosity increases to maintain a more or less constant fraction of the Eddington limit luminosity and maintain β near the preferred value.

Post-Main Sequence Evolution— Mixing and Nucleosynthesis

Following exhaustion of hydrogen in the center of stars, the inner regions contract to ignite a hydrogen burning shell. During the main sequence, much of the inner part of the star had its carbon and oxygen converted to nitrogen. When the star bifurcates into a contracting core and an expanding envelope, the inner boundary of the convective envelope maintains a more or less constant temperature after the star has reached the red-giant part of the Hertzsprung-Russell diagram (i.e. after it has finished crossing the Hertzsprung gap). As a mass variable, the inner convective envelope boundary has come very close to the mass of the hydrogen shell source. Since this shell source is at the inner edge of the hydrogen depleted zone and hydrogen burning during the main sequence reached much further out, the products of the main sequence hydrogen burning are incorporated into the convective envelope – this primarily results in an enhancement of the abundance of nitrogen.

The star undergoes core contraction/envelope expansion until helium ignites in the center. There is then a period of core helium burning which lasts until helium exhaustion. The star resumes its core contraction/envelope expansion with a condition of just the helium shell source. When the helium consumption eats out to the hydrogen rich layers, a two-shell source configuration forms. One of the first things that happens is for a second stage of dredge-up to take place with further mixing of CNO products to the stellar surface.

The figure at the left shows the processes leading to the first and second dredge-up phases.



The Two-Shell Source Thermal Instability – Thermal Pulses

It was discovered by Schwarzschild and Härm(1965ApJ...142...655S) that the combination of the hydrogen and helium shell sources is subject to an instability due to the thinness of the helium shell source. The sketches below show an idealized temperature structure of the helium shell source along with a perturbation to its temperature distribution:

